RICE UNIVERSITY

Experimental study of the effect of commercial dispersants on the precipitation, aggregation and deposition of asphaltenes

by

Ariana Amparo Meléndez Álvarez

A THESIS SUBMITTED
IN PARTIAL FULFILLMENT OF THE
REQUIREMENTS FOR THE DEGREE

Master in Science

APPROVED, THESIS COMMITTEE

Francisco M. Vargas, Assistant Professor
Chair, Chemical and Biomolecular Engineering

Sibani Lisa Biswal, Associate Professor,
Materials Science and Nano Engineering
Chemical and Biomolecular Engineering

Rafael Verduzco, Assistant Professor,
Chemical and Biomolecular Engineering

Scott Wellington, Distinguished Faculty Fellow
Chemical and Biomolecular Engineering

HOUSTON, TEXAS
November 2015

RICE UNIVERSITY

Experimental study of the effect of commercial dispersants on the precipitation, aggregation and deposition of asphaltenes

by

Ariana Amparo Meléndez Álvarez

A THESIS SUBMITTED
IN PARTIAL FULFILLMENT OF THE
REQUIREMENTS FOR THE DEGREE

Master in Science

APPROVED, THESIS COMMITTEE

Francisco M. Vargas, Assistant Professor
Chair, Chemical and Biomolecular Engineering

Sibani Lisa Biswal, Associate Professor,
Materials Science and Nano Engineering
Chemical and Biomolecular Engineering

Rafael Verduzco, Assistant Professor,
Chemical and Biomolecular Engineering

Scott Wellington, Distinguished Faculty Fellow
Chemical and Biomolecular Engineering

HOUSTON, TEXAS
November 2015

RICE UNIVERSITY

Experimental study of the effect of commercial dispersants on the precipitation, aggregation and deposition of asphaltenes

by

Ariana Amparo Meléndez Álvarez

A THESIS SUBMITTED
IN PARTIAL FULFILLMENT OF THE
REQUIREMENTS FOR THE DEGREE

Master in Science

APPROVED, THESIS COMMITTEE

Francisco M. Vargas, Assistant Professor
Chair, Chemical and Biomolecular Engineering

Sibani Lisa Biswal, Associate Professor,
Materials Science and Nano Engineering
Chemical and Biomolecular Engineering

Rafael Verduzco, Assistant Professor,
Chemical and Biomolecular Engineering

Scott Wellington, Distinguished Faculty Fellow
Chemical and Biomolecular Engineering

HOUSTON, TEXAS
November 2015

ABSTRACT

Experimental study of the effect of commercial dispersants on the precipitation, aggregation and deposition of asphaltenes

by

Ariana A. Melendez Alvarez

Asphaltene precipitation and subsequent deposition is a potential flow assurance problem for the oil industry nowadays. Moreover, because oil production is moving to more difficult production environments – e.g. deeper waters – or is focusing on extracting residual oil using enhanced oil recovery techniques, the significant changes of pressure, temperature and/or composition can aggravate asphaltene deposition problems. One of the most common strategies to prevent or at least reduce asphaltene deposition is the utilization of chemical additives. However, there are still several unresolved challenges associated with the utilization of these chemicals: First, the experimental conditions and results obtained in the lab are not always consistent with field observations. Also, in some cases these chemical additives seem to worsen the deposition problem in the field. Therefore, there is a clear need to revisit the commercial techniques used to test the performance of asphaltene inhibitors and to provide a better interpretation of the results obtained.

In this work, a technique based on NIR spectroscopy is presented to evaluate the performance of three commercial asphaltene dispersants. The results are also

validated using a digital optical microscope. This technique is faster and more reproducible compared to available methods such as Asphaltene Dispersion Test (ADT) and Solid Detection System (SDS). Also, unlike the ADT test, the proposed method can evaluate the performance of the dispersants in a wide range of temperatures and compositions. The chemical additive dosage, aging time and temperature effect on asphaltene aggregation process are also discussed in this manuscript.

A new system to study asphaltene deposition on metal surfaces that offers advantages over capillary systems was developed. This new apparatus is based on a column packed with carbon steel spheres. The current version of this device operates at ambient pressure and has potential for the fabrication of a high-pressure system in the near future.

The work presented in this dissertation will contribute to a better understanding of the variables that affect the performance of asphaltene dispersants, and the true effect these chemicals have on the complex multi-step mechanism of asphaltene precipitation, aggregation and deposition.

Acknowledgments

This research was possible thanks to the generous support of Abu Dhabi National Oil Company (ADNOC) Research and Development Oil Subcommittee.

I wish to express my deep gratitude to Professor Francisco M. Vargas, for being an excellent mentor and advisor. I am very grateful and honored for the confidence that he devoted to my work. His constant positive attitude and his ability to inspire and encourage those around him were vital to the completion of this work. I am deeply thankful for his support.

I also appreciate the time provided by other members of my thesis committee, Professor Sibani Lisa Biswal, Professor Rafael Verduzco and Professor Scott Wellington.

I am very grateful to Dr. Miguel García-Bermudes for his contribution to this work, his continuous guidance and patience, permanent collaboration and overall valuable friendship.

I am also very grateful to Dr. Mohammad Tavakkoli, for his permanent advice and guidance, for all the discussions on the asphaltene problematic, for his collaboration in the phases of this research project and for being a daily example of hard work and dedication.

I would like to thank all the Vargas group members for making the Vargas Laboratory a great place to work. I would like to thank Dr. Rocío Doherty for her

constant encouragement and for permanently taking care of all the group members and making us feel at home.

I would like to thank the current and former staff of the Chemical and Biomolecular Engineering department at Rice.

I am also grateful to Dr. Adria Baker, from the OISS at Rice, for her work to make all international students feel welcome at Rice.

My appreciation goes to my excellent friends Paola Andrea Díaz Porras and Diana Paola Agudelo for their unconditional friendship and their constant support.

I am deeply thankful to all my family members for their constant support and unconditional love. I am especially thankful to my aunt, Asceneth Álvarez, for being a source of happiness and laughter, to my godmother Luz Dary Fernández for her wisdom and assertive advice and to my friend Stella Goldstein for her permanent guidance and support.

And last but most importantly, I express my endless gratitude to my parents Amparo Alvarez and Gabriel Ricardo Vargas, to whom this dissertation is dedicated. They have been a source of encouragement, constant support and unconditional love. They have always been an example of hard work and resilience. No words can express how honored I feel for having them in my life, for helping me to overcome difficulties and for giving me motivation to complete this work.

Contents

Acknowledgments ..... **iv**

Contents ..... **vi**

List of Figures ..... **viii**

List of Tables ..... **xii**

List of Equations ..... **xiv**

Nomenclature ..... **xv**

Introduction **1**

1.1. Thesis motivation 1

1.2. Objectives 2

1.3. Thesis structure 3

Asphaltenes in crude oil systems **4**

2.1. Oil Characterization 4

2.2. Asphaltene Properties and Economic Impact in Oil Production 5

2.3. Mechanism for Asphaltene Deposition 7

2.4. Asphaltene Deposition Control 8

2.4.1. Physical Deposits Removal 8

2.4.2. Solvent Washes 9

2.4.3. Chemical Treatment 9

Asphaltene Inhibitors and Asphaltene Deposition Evaluation Techniques **13**

3.1. Asphaltene Commercial Inhibitors Evaluation 13

3.1.1. Asphaltene Dispersion Test - ADT 13

3.1.2. Solid Detection Systems - SDS 15

3.1.3. Direct Method 18

3.1.4. Indirect Method 18

3.2. Asphaltene Deposition Experimental Determination - Testing Procedures 20

3.2.1. Microfluidic Capillary Systems 21

3.2.2. Organic solid deposition cell (OSDC) 23

3.2.3. Limitations of the Asphaltene Deposition Existing Techniques 24

Asphaltene Inhibitors Evaluation 26
4.1. Materials 26
4.1.1. Model Oil Preparation 27
4.2. Commercial Asphaltene Dispersants Effect on Asphaltene Aggregation 28
4.2.1. Asphaltene Dispersion Test - ADT Experimental Procedure and Results 31
4.2.2. Direct method Experimental Procedure 34
4.2.3. Direct Method Results 36
4.2.3.1. Effectiveness of Commercial Asphaltene Dispersants 37
4.2.3.2. Effect of Dosage 43
4.2.3.3. Effect of Aging Time 47
4.2.3.4. Effect of Temperature 51
4.2.3.5. Definition of Dispersive Performance 56
4.3. Effect of Commercial Asphaltene Dispersants on the Precipitation of Asphaltene 59
4.3.1. Experimental Procedure for the Indirect Method 59
4.3.2. Indirect Method Results 60
4.4. Effect of Commercial Asphaltene Dispersants on the Deposition of Asphaltenes 68
4.4.1. Development of a New System for the Asphaltene Deposition Evaluation 68
4.4.2. Experimental procedure and results 78
Conclusions and Recommendations 87
5.1. Conclusions 87
5.2. Recommendations 91
References 94
Appendix A. Direct Method Correction of the Dilution Effect 101

List of Figures

Figure 2-1. Characterization for SARA analysis. Reproduced from Wang[4] 5

Figure 2-2. Proposed mechanism for asphaltene precipitation, aggregation and aging. The double green arrow represents reversibility.[26] 8

Figure 3-1. ADT for Crude Oil S treated with 70 and 500 ppm of dispersant 9 at 0 and 24 hours..... 15

Figure 3-2. Results for AOP measurement using NIR and HPM at 93°C for (a) Crude Oil A (b) Crude Oil A treated with 100 ppm dispersant 9 (c) Crude Oil A vs. Crude Oil A treated with 100 ppm dispersant 9. 17

Figure 3-3. Deposition decrease as a function of the distance from the capillary entracnce at the end of the experiment with a flow rate of 10 µL min-1 . Taken from Boek et al.[57]..... 22

Figure 4-1. Results for crude oil A and crude oil S (a) Results for AOP measurement using NIR and HPM for Crude Oil A at 93°C (b) Direct spectroscopy results for Crude Oil S diluted with n-heptane and aged for 1 h at 25˚C..... 30

Figure 4-2. Direct spectroscopy results for crude oil S diluted with n-heptane and aged for 1 h at 25˚C. Normalized light intensity and corrected to remove the effect of dilution. 31

Figure 4-3. ADT Test results for Crude oil S treated with dispersants 8, 9 and 15 at 70 ppm and 500 ppm for aging times of 0 hours, 1 hour, 24 hours and 1 week..... 33

Figure 4-4. Direct method results for the crude oil S diluted with n-heptane and aged for 1 h at 25˚C. The ASD is 6.03%..... 37

Figure 4-5. Direct method results for the crude oil S with a 70-ppm dosage of different commercial dispersants, after mixing with heptane and aging for 1 h at 25˚C. (a) Dispersant 8 vs. Blank, 50-100 vol.% n-heptane, (b) Dispersant 8 vs Blank, 0-50 vol.% n-heptane. (c) Dispersants 8, 9 and 15 vs. Blank. The ASD are 6.03%, 5.31%, 6.82% and 3.21% for the blank, dispersant 8, 9 and 15, respectively. 41

Figure 4-6. Results of the direct method for the crude oil S, mixed with a 70-ppm dosage of dispersant 9, diluted with n-heptane and aged for 1 h at 25°C.42

Figure 4-7. Direct method results for crude oil S with *(a)* Dispersant 8 *(b)* Dispersant 9 (c) Dispersant 15 at different dosages, after mixing with n-heptane and aging for 1 h at 25°C. The ASD are 6.03%, 5.31%, 6.82%, 3.21%, for the blank, dispersant 8, 9 and 15 at 70 ppm and 2.43%, 0.502%, 0.017% for dispersant 8, 9 and 15 at 500 ppm, respectively. 44

Figure 4-8. Results of the direct method for the crude oil S with (a) Dispersant 8, 9 and 15 at 70 ppm (b) Dispersant 8,9, and 15 at 500 ppm, after mixing with heptane and aging for 1 h at 25°C. The ASD are 6.03%, 5.31 %, 6.82%, 3.21%, for the blank, dispersant 8, 9 and 15 at 70 ppm, and 2.43%, 2.62%, 0.46%, for dispersant 8, 9 and 15 at 500 ppm, respectively. 46

Figure 4-9. Results of the direct method for the crude oil S with (a) Blank (b) Dispersant 8 at 70 ppm (c) Dispersant 9 at 70 ppm, after mixing with heptane and aging for 1 h, 24 h and 2 weeks at 25°C. The ASD are 6.03%, 5.57% and 2.55% for the blank at 1 h, 24 h and 2 weeks, respectively. 5.31 %, 2.18%, 1.79% for dispersant 8 at 1 h, 24 h and 2 weeks, respectively. 6.82%, 3.20%, 4.27% for dispersant 9 at 1 h, 24 h and 2 weeks respectively.....49

Figure 4-10. Detection of asphaltene precipitation after 1 hour, 24 hours and 2 weeks aging time for crude oil S without adding dispersants, and with dispersants 8 and 9 at 70 ppm dosage. Time axis in log scale. 51

Figure 4-11. Results of the direct method for the crude oil S for (a) Blank (b) Dispersant 8 at 70 and 500 ppm (c) Dispersant 8 at 70 and 500 ppm, after mixing with heptane for 24 hours at 25°C and 70°C. The ASD are 2.44%, 3.34%, 4.68%, 6.20%, 5.98%, 1.89% for blank 25°C, blank 70°C, dispersant 8 at 70 ppm and 500 ppm at 25°C, dispersant 8 at 70 ppm and 500 ppm at 70°C, respectively.....54

Figure 4-12. Results of the direct method for the crude oil S for (a) Dispersant 9 at 25°C (b) Dispersant 9 at 70°C, after mixing with heptane for 24 hours. The ASD are 5.57%, 3.20% for the blank and Dispersant 9 at 25°C and 3.34%, 2.11% for the blank and Dispersant 9 at 70°C, respectively.....55

Figure 4-13. Indirect method results for crude oil S with (a) Dispersant 8 and (b) Dispersant 9 at 70 ppm dosage (c) Dispersant 8 at 70 ppm and 500 ppm, after mixing with heptane and aging for 24 h at 25°C. The ASD are 2.15% for

the blank, 1.51%, 1.4% and 1.0%, for dispersant 8 and dispersant 9 at 70 ppm, and dispersant 8 at 500 ppm respectively. 63

Figure 4-14. Indirect method results reported as normalized light intensity vs. crude oil vol. % and heptane vol. % for crude oil S with (a) Dispersant 8 at 70 ppm (b) Dispersant 9 at 70 ppm dosage (c) Dispersant 8 at 70 ppm and 500 ppm, after mixing with heptane and aging for 24 h at 25˚C. The ASD are 2.15% for the blank, 1.51%, 1.4% and 1.0% for dispersant 8 and dispersant 9 at 70 ppm and dispersant 8 at 500 ppm respectively. 65

Figure 4-15. Results for crude oil S with a 2000-ppm dosage of dispersant 9, after mixing with heptane and aging for 24 h at 25˚C. (a) Direct method. The ASD are 3.17% and 3.27% for the blank and dispersant 9 respectively. (b) Indirect method. The ASD are 1.73% and 2.32% for the blank and dispersant 9 respectively. 67

Figure 4-16. Connection from Tee junction inmerse in the ultrasonic water bath to the inlet of the column. (a) Cooper cooling coil. (b) Water recirculation system. 72

Figure 4-17. System leaks while in operation using Chemical resistant PFA straight connectors. 90-10 n-heptane to model oil A ratio, 12 ml/hr 74

Figure 4-18. Column Detail. (a) PTFE Column (b) Detailed Nylon straight connector (c) PTFE mesh location 75

Figure 4-19. Novel system to probe asphaltene deposition at ambient conditions and under dynamic conditions. (a) The system is composed by multiple sections. Here the empty middle section is highlighted. (b) Each section was filled with carbon steel spheres, to increase the surface area and the amount of asphaltene that can potentially deposit. (c) A blend of crude oil and n-heptane flown through and the asphaltene deposited was collected and quantified. 76

Figure 4-20. Schematic of the novel system to probe asphaltene deposition at ambient conditions and under dynamic conditions. 77

Figure 4-21. Novel system to probe asphaltene deposition at ambient conditions and under dynamics conditions. 77

Figure 4-22. Bottom adapter – Reducer connector. Visual inspection after test completion. Crude oil S evaluated at 70-30 precipitant to oil ratio, 12 ml/h and 6h treated with (a) 100 ppm of dispersant 8 (b) 500 ppm of dispersant 9.....82

Figure 4-23. Bottom section PTFE Mesh visual observation after test completion. Crude oil S evaluated at 70-30 precipitant to oil ratio, 12 ml/h and 6h treated with (a) 100 ppm of dispersant 8 (b) 500 ppm of dispersant 9.....82

Figure 5-1. HPHT Stainless steel column for the study of asphaltene deposition. 93

Figure A-1. Raw spectroscopy data for the direct method applied to a crude oil with asphaltene concentration of 2.8 wt. % diluted with n-heptane (C_7) and aged for 1 hour Novel system to probe asphaltene deposition at ambient conditions and under dynamic conditions.....101

Figure A-2. (Figure 4-1 (b)) Direct spectroscopy results for Crude Oil S diluted with n-heptane and aged for 1 h at 25°C. 107

Figure A-.3. (Figure 4-2) Direct spectroscopy results for Crude Oil S diluted with n-heptane and aged for 1 h at 25°C. Normalized light intensity and corrected to remove the effect of dilution.. 108

List of Tables

Table 3-1 Crude oil S properties at 20ºC and 1 atm 15

Table 3-2. Crude oil A properties at 15ºC and 1 atm 18

Table 4-1. ADT for Crude Oil S treated with dispersants 8, 9 and 15 at 70 and 500 ppm. 34

Table 4-2. Detection of asphaltene precipitation of crude oil S with a 70-ppm dosage of different commercial dispersants, after mixing with heptane and aging for 1 h at 25°C 42

Table 4-3. Detection of asphaltene precipitation of crude oil S with 500 ppm dosage of different commercial dispersants, after mixing with heptane and aging for 1 h at 25°C 47

Table 4-4. Detection of asphaltene precipitation of crude oil S threated with different commercial dispersants at 70 ppm, after mixing with heptane and aging for 1 h, 24 h and 2 weeks at 25°C 50

Table 4-5. Dispersive performance efficiencies for Dispersants 8, 9 and 15 at different dosages, temperatures and aging time conditions. Efficiency and Maximum efficiency* reported. 57

Table 4-6. Material composition of the carbon steel spheres 73

Table 4-7. Evaluation of the operation conditions with model oil A with an asphaltene content of 1 wt. % *Result for a single experiment 79

Table 4-8. Asphaltene accumulation on the system components for the model oil A evaluated at 70-30 model oil to precipitant ratio, 12 ml/h and 6h 80

Table 4-9. Dispersant effect on asphaltene deposition for Crude Oil S evaluated at 70-30 crude oil to precipitant ratio, 12 ml/h and 6h 81

Table 4-10. Dispersant dosage effect on asphaltene deposition for Crude Oil S evaluated at 70-30 crude oil to precipitant ratio, 12 ml/h and 6h 83

Table 4-11. Asphaltene accumulation (%) on the system components for treated and untreated crude oil S evaluated at 70-30 crude oill to precipitant ratio, 12 ml/h and 6h 84

Table A-1. Calculation of the dilution effect caused by the addition of n-heptane (C7) to the Crude Oil S 103

Table A-2. Calculation of the corrected absorbance values after removing the effect of dilution at 1100 nm 104

Table A-3. Data processing of the light intensity before and after the removal of the dilution effect for Crude Oil S at 25°C and 1 hour aging time 105

Table A-4. Direct spectroscopy results for Crude Oil S diluted with n-heptane and aged for 1 h at 25 °C 106

Table A-5. Direct spectroscopy results for Crude Oil S diluted with n-heptane and aged for 1 h at 25°C. Normalized light intensity and corrected to remove the effect of dilution 107

List of Equations

Equation 4-1. Dispersive Performance Efficiency 56

Equation 4-2. Area under the curve calculation for DPE 56

Equation 4-3. Reynolds number for a packed bed 69

Equation 4-4. Void fraction definition 69

Equation 4-5. Superficial velocity definition 70

Nomenclature

ADT	Asphaltene Dispersion Test
AOC	Asphaltene Onset Concentration
AOP	Asphaltene Onset Pressure
DCM	Dichloromethane
DPE	Dispersive Performance Efficiency
ETFE	Ethylene tetrafluoroethylene
FEP	Fluorinated ethylene propylene
GOM	Gulf of Mexico
HPHT	High Pressure High Temperature
HPM	High Pressure Microscopy
ID	Inner Diameter
NIR	Near Infrared
OD	Outer Diameter
PEEK	Polyetheretherketone
PFA	Perfluoroalkoxy
PTFE	Polytetrafluoroethylene
SEM	Scanning Electron Microscopy

Chapter 1

Introduction

1.1. Thesis motivation

One of the most common strategies to prevent or at least reduce asphaltene deposition is the utilization of chemical additives. However, there are still several unresolved challenges associated with the utilization of these chemicals: First, the experimental conditions and results obtained in the lab are not always consistent with field observations. Also, in some cases these chemical additives seem to worsen the deposition problem in the field. Therefore, there is a clear need to revisit the commercial techniques used to test the performance of asphaltene inhibitors and to provide a better interpretation of the results obtained.

The aim of this study is to contribute to the understanding of the effect of commercial inhibitors on the precipitation, aggregation and deposition of asphaltenes. Also, since the ultimate goal of using these chemicals is to reduce the

amount of asphaltene deposit obtained in production tubing, it is greatly desirable to study the performance of these chemicals to reduce actual deposition.

The screening of inhibitors using ADT is not a good tool to select asphaltene deposition inhibitors. The so-called “good inhibitors-dispersants” have the potential to increase asphaltene deposition rate. Thus, one of the motivations of this work is the development of a new system to study asphaltene deposition.

The ability to identify appropriate chemical inhibitors to prevent asphaltene deposition is crucial in the flow assurance effort. The cost associated with asphaltene deposition prevention and remediation is in the order of millions of dollars per year. Thus, the adequate selection of chemical treatments designed to prevent asphaltene deposition can save the expense of injecting chemical inhibitors or dispersants when not required or when they do not represent the best option for a particular well.

1.2. Objectives

Three main objectives have driven the work presented in this dissertation:

1. Revisit the commercial techniques used to test the performance of asphaltene inhibitors.
2. Study the effect of commercial asphaltene inhibitors on asphaltene precipitation, aggregation and deposition phenomena.

3. Develop a new methodology to study asphaltene deposition and test the performance of commercial asphaltene inhibitors.

1.3. Thesis structure

In this work, an overview of the effect of asphaltene commercial inhibitors on asphaltene precipitation, aggregation and deposition is provided. A brief background on asphaltenes and its impact in oil production is presented.

Chapter 2 presents a review of asphaltenes. The definition of asphaltenes, characterization, and their impact in oil production, asphaltene deposition mechanism and types of asphaltene deposition control are discussed.

Chapter 3 presents an overview of asphaltene commercial inhibitors techniques of evaluation and asphaltene deposition experimental determination techniques that are available.

Chapter 4 presents two techniques based on NIR spectroscopy to evaluate the performance of three commercial chemical inhibitors and their effect on asphaltene precipitation and aggregation. Commercial chemical inhibitors dosage, aging time and temperature effect on asphaltene aggregation process are presented. In addition, a new system to evaluate asphaltene deposition on metallic surfaces and the effect of commercial chemical inhibitors on asphaltene deposition are presented.

In Chapter 5 conclusions and recommendations for future work are presented.

Chapter 2

Asphaltenes in crude oil systems

2.1. Oil Characterization

Crude oil is a very complex system that contains more than 100.000 different molecules.[1, 2] Therefore, these components are classified in terms of their solubility. The SARA analysis first developed by Jewell et al.[3] classify the oil components in four groups (Saturates, Aromatics, Resins and Asphaltenes). Asphaltenes are the least soluble component in the crude oil system. Once they are removed from oil, the remaining part, which is composed of saturates, aromatics, and resins, is called maltene. Figure 2-1 presents the classification of crude oil based on the SARA analysis.

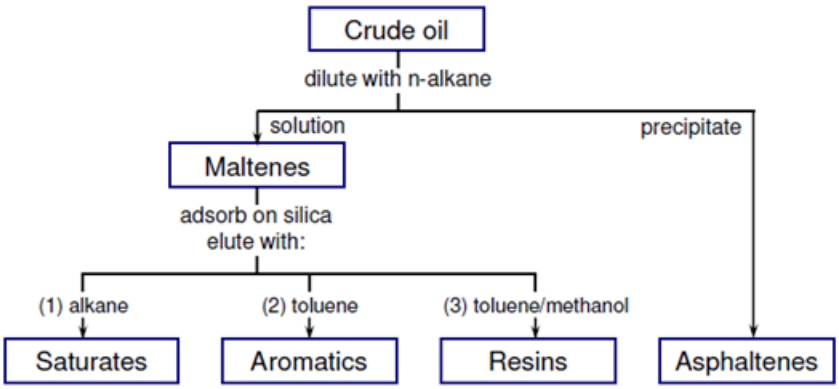

Figure 2-1. Characterization for SARA analysis. Reproduced from Wang[4]

2.2. Asphaltene Properties and Economic Impact in Oil Production

Asphaltenes are defined as a poly-disperse distribution of the heaviest and most polarizable fraction of crude oil.[2] They are defined in terms of their solubility, being completely miscible in aromatic solvents, such as benzene, toluene or xylenes, but insoluble in light paraffinic solvents, such as n-pentane or n-heptane.[4] Other strong asphaltenes precipitants are alcohols, water, and gases such as methane, nitrogen and CO_2. The latter can prevent asphaltene precipitation depending on the operating conditions.[2]

Asphaltene characterization,[5–8] chemical structure and physicochemical properties are still under investigation.[9] Precipitation and deposition of asphaltenes are phenomena induced by changes in pressure, temperature and composition.[10–12] During pressure depletion at low enough pressures, asphaltene precipitation onset is reached and asphaltenes begin to precipitate.[10] At these conditions, oil expands and becomes a poor asphaltene solvent. Once asphaltenes precipitate, a multistep

process that involves aggregation, diffusion, advection and deposition of asphaltene aggregates begins.[10] The mechanism for asphaltene formation will be discussed in section 2.3. Oil production from deeper waters[2] and enhanced oil recovery operations such as carbon dioxide injection,[13] tend to worsen asphaltene deposition. Potential solutions for asphaltene deposition include physical deposits removal,[11,14] solvent washes[11,14,15] and chemical treatment with appropriate additives. [14, 16–18]

Asphaltene deposition in reservoirs, wells, and facilities severely impacts oil production economics.[19] It can cause formation damage and wellbore plugging that can require expensive treatment and clean-up procedures,[16] and in extreme cases, it can cause a wellbore to be completely plugged.[10,20] For Gulf of Mexico oil fields the economic impact associated with this problematic has been estimated in USD $70 M per well (wet tree) when well shut-in for ring interventions is required. [21] If the deposition occurs in the surface controlled subsurface safety valve (SCSSV), the cost increases to USD $100 M per well. Downtime losses based on 10,000 BBL per day production and oil price of USD $60 per barrel, can reach up to USD $600 k a day. Replacing a lost well with a side track raises the cost to around USD $150 M. [21] Chemical additive injection for typical Gulf of Mexico production of 10,000 BBL/day represents costs estimated between USD $330 k and USD $390 k per year. [21] For Middle Eastern fields, chemical additive injection represents costs ranging from USD $31 k to USD $46 k per well per year. [22]

The cost of installing and maintaining asphaltene mitigation equipment and chemicals is in the millions of dollars per year. Differentiation between cases that requiring well intervention from those with minimal or no wellbore deposition

could prevent the installation of unnecessary equipment and the injection of chemical inhibitors when they are not needed,[2,23] as well as aiding in the development of improved chemicals for prevention of wellbore deposition problems.[2]

During design of oil production and transportation facilities the possibility for asphaltene deposition in wellbores and flow lines is a major concern, especially in deep-water environments.[2,24]Asphaltene deposits can cause formation damage and wellbore plugging that require expensive treatment and clean-up procedures.[16] In some extreme cases a wellbore can be completely plugged.[10] Asphaltene deposits can be removed by the addition of large and costly amounts of aromatic solvents.[25]

2.3. Mechanism for Asphaltene Deposition

Asphaltene aggregates morphology was studied by Vargas et al.[26] using Scanning Electron Microscopy (SEM). Based on experimental observations and previous work reported by Mullins,[27,28] Vargas et al.[26] proposed a conceptual multistep mechanism to describe asphaltene precipitation, aggregation and deposition phenomena. Figure 2-2 presents the conceptual mechanism. According to this process, asphaltene precipitation generates small particles called “primary particles” that are on the order of a few hundred nanometers – about 100 to 400 nm in size. [29] Once the primary particles are formed, they aggregate and form micro-aggregates. As micro-aggregates age their structure rearranges and becomes more compact and solid-like. The first two steps of this process are below the detection

limit of commercial instruments to measure asphaltene onset pressure (AOP) as will be discussed in section 3.1.

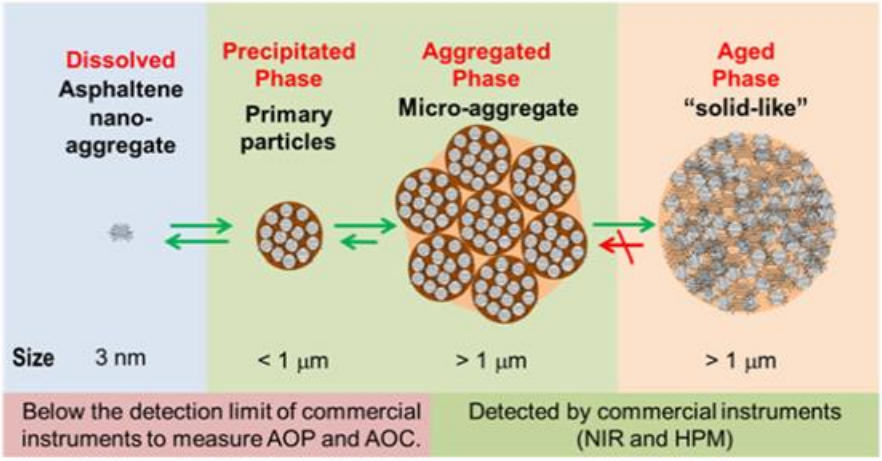

Figure 2-2. Proposed mechanism for asphaltene precipitation, aggregation and aging. The double green arrow represents reversibility.[26]

2.4. Asphaltene Deposition Control

As was mentioned in section 2.2, potential solutions for asphaltene deposition include physical deposits removal,[11,14] solvent washes[11,14,15] and chemical treatment with appropriate additives. [14, 16–18]

2.4.1. Physical Deposits Removal

Some of the remedial methodologies recommended to remove asphaltene deposits are:[14,30,31]

- Wireline cutting: This method can be time consuming and impractical[30,31]

- Pigging: This can cause some tube pipe material loss and scrapes tubes and piping surfaces
- Hydroblasting: Cleaning technique that uses high-pressure water stream to remove deposits is abrasive/erosive
- Drilling

2.4.2. Solvent Washes

Asphaltene deposits can be removed using solvents. Light aromatic compounds such as benzene, xylene and toluene are used. This type of treatment is effective in removing asphaltene deposits, but it is expensive[30] and has risks associated. These compounds are volatile and have a low flash point; thus, at low temperatures under normal conditions they can form an ignitable vapor. In addition, there are environmental restrictions associated with the use of these types of solvents. This method requires the use of large amounts of solvents, as well as high frequency of treatment.[14, 31, 32]

2.4.3. Chemical Treatment

One of the most common strategies to mitigate asphaltene deposition consists of using chemical additives.[33] They are designed to reduce asphaltene aggregation and to keep asphaltene particles dispersed in the liquid phase.[34–36] Chemical additives that are injected directly into the reservoir fluid as it travels through the wellbore to prevent asphaltene deposition are called asphaltene deposition inhibitors.

Extensive research has been conducted to elucidate the variables that affect additives performance.[17,19,37–40] It has been reported that asphaltene characteristics,[38,41,42] solvent condition,[17,40,43,44] additive structure,[37,38,44] and additive amount adsorbed on asphaltenes [6,40,43] influence additive performance.

These chemical additives can perform as asphaltene dispersants or asphaltene inhibitors. In the case of dispersant additives, it is accepted that dispersant interaction with asphaltenes decreases the aggregates size of precipitated asphaltene and/or hinders possible subsequent aggregation.[45,14] However, in other cases the dispersants seem to promote the aggregation.[40] The study of asphaltene dispersant additives has shown that additives can have different performance, acting as stabilizers, enhance aggregation or have no effect.[16] Thus, the use of asphaltene dispersants would not necessarily improve the asphaltene stability in oil.[46]

A large variety of asphaltene dispersants has been studied for the purpose of finding cost efficient, safer and more environmentally friendly alternatives. Some of the different classes of low molecular weight, nonpolymeric asphaltene dispersants are the following:[47] very low polarity alkyl aromatics, alkylaryl sulphonic acids, phosphoric esters and phosphonocarboxylic acids, sarcosinates, ethercarboxylic acids, aminoalkylenecarboxylic acids, imidazolines and alkylamide-imidazolines, alkylsuccinimides, alkylpyrrolidones, fattyacid amides and their ethoxylates, fatty esters of polyhydric alcohols, ion-pair salts of imines and organic salts and ionic liquids. The most studied inhibitors that efficiently disperse asphaltenes include; n-

alkyl-aromatic sulfonic acids, [47] chemical structures based on N-aryl amino alcohols and boronic acids[43] and polyisobutylene succinimides[48], which are standard dispersants for motor oils. There are many commercial inhibitors available, but their compositional information is usually unavailable.

Asphaltene dispersants in general contain a polar group that attaches to the asphaltene surface and an alkyl group that blocks other asphaltene molecules. The polar group generally contains etheroatoms such as oxygen, nitrogen or phosphorous.[14] The nonpolymeric asphaltene dispersants polar and/or aromatic head groups with long alkyl tails interact with aggregated asphaltene molecules. The polarity of the outside of the aggregate changes with the help of the long alkyl chains, and the aggregate is more similar to crude oil, and thus, it is dispersible in crude oil.[47] The types of interactions between asphaltene dispersants and asphaltenes are:[47]

- π – π interaction between unsaturated or aromatic groups and asphaltene molecules.
- Acid – base interactions
- Hydrogen bonding
- Dipole – dipole interactions
- Complexing of metal ions

Chemical additives efficiency is typically measured in terms of delay in the detection of asphaltene precipitation.[17,49,50] Some methodologies such as microscopy,[11,51] polarized light microscopy,[52] solid detection system,[17] filtration,,[39] filter drop spreading method[49,53] and spectroscopy[54] have been used to evaluate the performance of chemicals that reduce or prevent asphaltene deposition problems. One of the most common and widely used commercial techniques is the asphaltene dispersion test (ADT).[13] Details of this technique will be discussed in section 3.1.1.

Despite the widespread availability of these chemicals, several unresolved challenges associated to their utilization remain.[40] These include the disagreement between results obtained in the laboratory and in the field. Additionally, in some cases, the inhibitors were found to increase deposition and in other cases they had no effect.[16] This urges the need to investigate the commercial techniques used to test the performance of asphaltene inhibitors.

Chapter 3

Asphaltene Inhibitors and Asphaltene Deposition Evaluation Techniques

3.1. Asphaltene Commercial Inhibitors Evaluation

Tests used to evaluate chemical additives-asphaltene inhibitors mentioned in section 2.4.3 such as microscopy[11,51] and spectroscopy[54] are designed for laboratory environments.[46] In the case of solid detection systems, the system is bulky and fragile and therefore, unsuitable for field use.[17] As such most of the tests performed in the field are based on precipitation tests.[46]

3.1.1. Asphaltene Dispersion Test - ADT

To evaluate the tendency of asphaltenes to precipitate and the efficiency of chemical additives, ADT uses normal gravimetric sedimentation measured over a period of time after diluting the oil with an asphaltene precipitant.[13] Figure 3-1

presents typical results for ADT for untreated and treated crude oil S whose properties are reported in Table 3-1 with a chemical additive at two different dosages after 24 hours. According to this technique, the sample that shows the least amount of sediment represents where asphaltenes are most stable. In other words, ADT ranks the efficiency of the chemical additives based on their ability to disperse the asphaltene aggregates, which in turn reduces the terminal velocity of these particles and, consequently, the amount of sediment obtained.[13] However, the amount of sediment is not necessarily a good indicator of the ability of these chemicals to prevent asphaltene precipitation or deposition. There is experimental evidence suggesting that when asphaltenes precipitate they form very small particles – about 100 to 400 nm in size[29] and, although precipitation has already occurred, the amount of sediment obtained even after 24 hours is very small because of the small particle size. In addition, visual observation is more prone to uncertainties due to the variability in perception of different people who perform the experiment. This technique also requires the addition of n-heptane to the oil sample, at a ratio of 40 parts of n-heptane per part of oil (97% heptane or more). Aside from the significant amount of solvent required, this high dilution may not be representative of the conditions in which asphaltenes precipitate and aggregate in real systems.

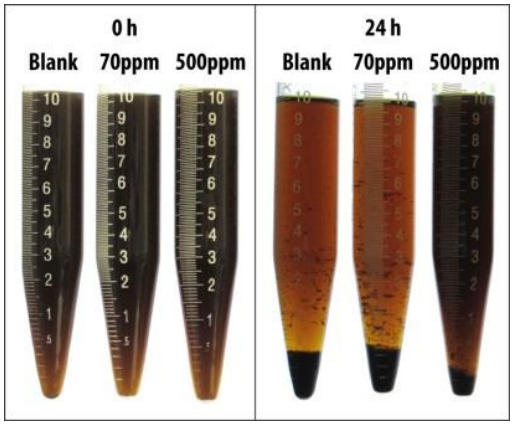

Figure 3-1. ADT for Crude Oil S treated with 70 and 500 ppm of dispersant 9 at 0 and 24 hours

Table 3-1 Crude oil S properties at 20°C and 1 atm

Property	Value
Density (g/cm^3)	0.843
Molecular weight (g/mol)	193
Viscosity (cP)	9.5
Saturate (wt %)	66.26
Aromatic (wt %)	25.59
Resin (wt %)	5.35
n-C_5 Asphaltene (wt %)	2.8
n-C_7 Asphaltene (wt %)	1.1

3.1.2. Solid Detection Systems - SDS

The solid detection system (SDS) is another technique used by service laboratories to evaluate the stability of asphaltenes. Unlike the ADT test, SDS can analyze live oil samples at high pressure and high temperature (HPHT) to determine asphaltene onset pressure (AOP) with and without the addition of asphaltene

dispersants. This instrument measures the transmittance of light at a fixed wavelength in the near infrared (NIR) region and provides high pressure-microscopy (HPM) images to detect and quantify asphaltene onset pressure (AOP) at a particular temperature and composition. The crude oil sample is loaded into the SDS cell and is stabilized at the temperature and pressure of interest. The fluid is then depressurized step-wise. During depressurization, the light transmittance that passes through the sample is measured and images using the HPM are recorded. Figure 3-2 (a) presents the SDS results obtained for crude oil A whose properties are reported in Table 3-2. According to this figure, the light transmittance increases as the pressure decreases from 8,000 to 3,500 psi. At a pressure below 3,500 psi the light transmittance starts to decrease. 3,500 psi is considered the AOP. HPM images show some particles even at high pressures but particles are more prominent and start to readily grow below the recorded AOP. The reported uncertainty for this measurement is about 200 psi. Figure 3-2 (b) shows the result for crude oil A treated with 100 ppm of commercial dispersant 9. In this case the AOP drops to 2,500 psi ± 200 psi. The AOP decrease can be clearly observed in Figure 3-2 (c) where transmittance curves for treated and untreated samples are compared. At this point, it is important to alert the reader that the shift in recorded AOP upon addition of the dispersant does not mean the thermodynamic stability of asphaltene was affected. This point will be further discussed in Section 4.1.

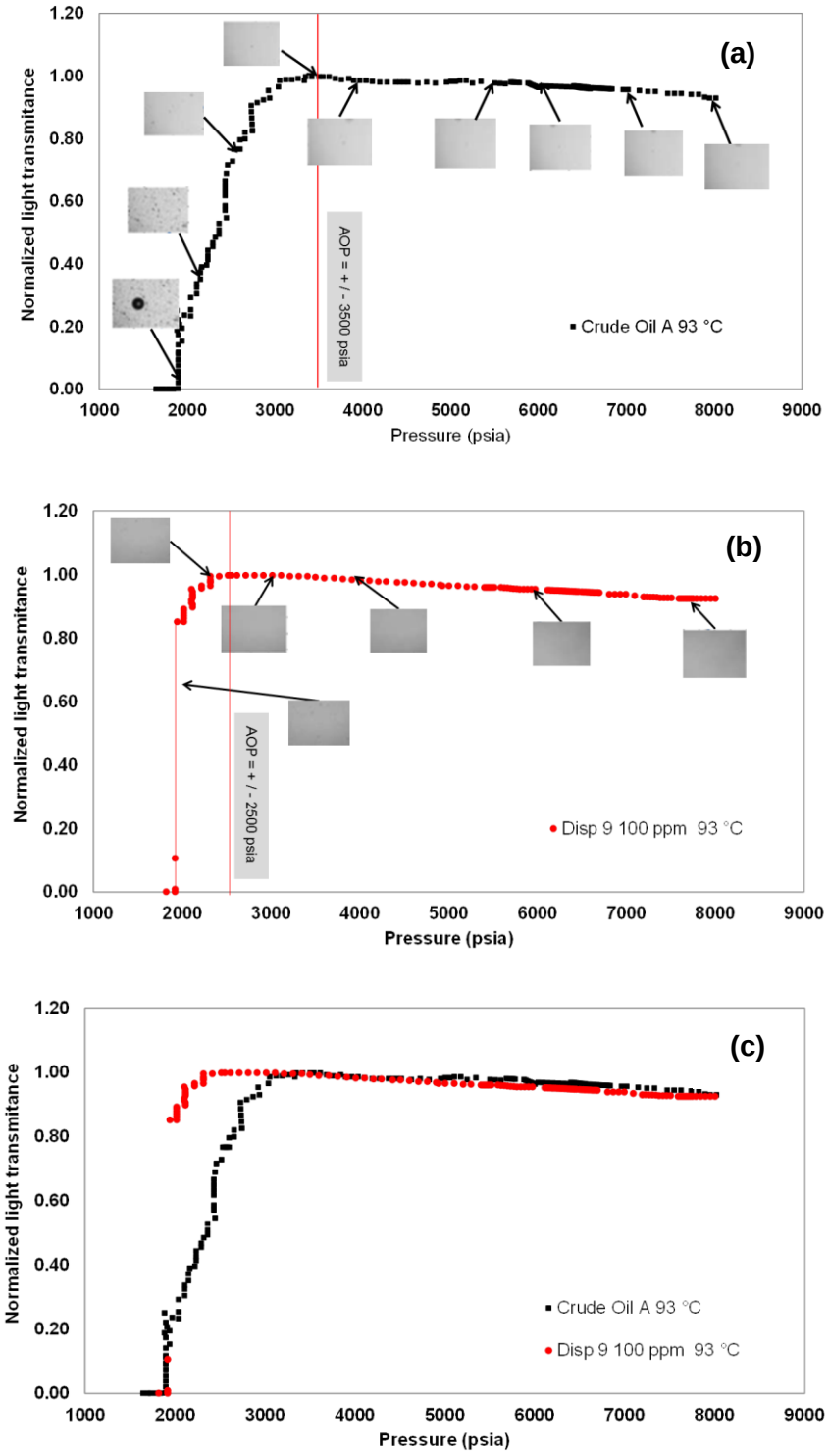

Figure 3-2. Results for AOP measurement using NIR and HPM at 93°C for (a) Crude Oil A (b) Crude Oil A treated with 100 ppm dispersant 9 (c) Crude Oil A vs. Crude Oil A treated with 100 ppm dispersant 9.

Table 3-2. Crude oil A properties at 15ºC and 1 atm

Property	Value
Density (g/cm^3)	0.763
Molecular weight (g/mol)	177
Viscosity (cP)	1.057
Saturate (wt %)	68.9
Aromatic (wt %)	21.8
Resin (wt %)	7.1
n-C_5 Asphaltene (wt %)	0.5

3.1.3. Direct Method

This method is a combination of gravimetric and spectroscopy techniques, which allows for the evaluation of treated and untreated crude oil samples at ambient conditions in order to study asphaltene aggregation phenomena. Similar to most techniques used for the detection of asphaltene precipitation, the "direct method" determines the onset of asphaltene precipitation by directly detecting the presence of asphaltene particles. The experimental procedure details will be presented in section 4.2.2.

3.1.4. Indirect Method

Due to the size detection limitation of direct techniques, the observed onsets of precipitation are in reality "onsets of asphaltene aggregation". Tavakkoli et al. and Vargas et al. [26,55] proposed a novel method referred to as the "indirect method" to measure the onset of asphaltene precipitation. This method is considered "indirect" because it is not based on the detection of asphaltene aggregates and therefore does not have the size limitations that direct techniques have. The indirect method shows

three main advantages over commercial methods that "directly" measure asphaltene precipitation. First, it measures asphaltene precipitation independently of aggregation and also quantifies the amount of precipitated asphaltenes –the absorbance of the supernatant fluid after centrifugation can be related to the amount of precipitated asphaltene using a proper calibration curve–. Second, it can be used with crude oils with asphaltene contents ranging from low (0.2 wt. %) to high (greater than 10%). Finally, the indirect method is more sensitive than commercial direct methods, since it can detect asphaltene particles as small as 100 nm.[29] Detection of yet smaller particles can occur if the centrifugation speed and/or centrifugation time are adjusted accordingly.

Because precipitation is measured independently of aggregation using the indirect method,[29] the chemical additive effect on asphaltene precipitation and aggregation phenomena can be independently studied. The indirect method is a combination of gravimetric and spectroscopic techniques. Details of this technique are presented in section 4.3.1 and can also be found in the work of Tavakkoli et al.[29]

The term "indirect" refers to the quantification of asphaltenes that remain in solution, after precipitation and centrifugation of the samples. The underlining principle of this method is that submicron particles that are not detected by NIR light-scattering techniques and optical microscopy can be settled down by high speed centrifugation. The removal of these particles affects the transmittance of the supernatant liquid, this in turn, can be used to detect the point of asphaltene precipitation.

3.2. Asphaltene Deposition Experimental Determination - Testing Procedures

The ability to predict the incidence and magnitude of asphaltene deposition in wellbores and flow lines is a key factor in the flow assurance effort.[2] When efforts to anticipate asphaltene deposition fail they represent significant costs in terms of remediation and production loss as mentioned in section 2.2. On the contrary, accurate prediction of deposition can enable differentiation of cases with substantially impaired production requiring well intervention from those with minimal or no wellbore deposition. This can save the expense of installing unnecessary equipment and injecting chemical additives when not needed as well as helping the development of improved chemicals for prevention of wellbore deposition problems. Asphaltene deposition is a complex process that depends on flow shear rate, surface type and characteristics, particle size, and particle surface interactions.[56]

Whereas asphaltene precipitation is a necessary condition for deposition, the real threat is the accumulation of asphaltene deposits on the production tubing, near the wellbore region, and on the surface and subsurface equipment. Due to technical difficulties and the high cost associated with the collection and analysis of reservoir fluids, most of the work reported in the literature for asphaltene deposition has been conducted at ambient pressure using dead oil samples. At ambient conditions, the precipitation and subsequent deposition of asphaltenes is achieved by the addition of a normal alkane, usually n-pentane or n-heptane.

Different configurations and geometries have been used to study asphaltene deposition; examples of these are described in the following section.

3.2.1. Microfluidic Capillary Systems

Boek et al. [57] studied asphaltene precipitation and deposition in microfluidic glass capillaries using optical microscopy under flow conditions in combination with measurement of the pressure drop in very low-Reynolds number flows.[57] This study allows direct visual observation of the deposition as a function of the distance from the capillary entrance, as well as the measurement of the pressure drop as a function of time.[57] From light microscopy it was observed that the amount of asphaltene deposited decreased with distance from the capillary inlet as shown in Figure 3-3.

Also, according to these studies the aggregation/deposition rates increase when increasing flow rate;[57] this is in agreement with the work on asphaltene aggregation in shear flow from Rahmani et al.[58] who observed that for early times, the largest aggregates are observed for the highest imposed shear rate.

Using a metal capillary, Broseta et al[59] calculated the effective hydrodynamic thickness of a deposited asphaltene layer in flow experiments, assuming a uniform thickness of the layer deposited. Wang et al. [24] studied the deposition of asphaltene on metallic surfaces using the homogeneous deposition hypothesis as well. However, the axial deposition profile is not necessarily uniform.[60] The series of experiments conducted by Wang et al[24] used a capillary flow loop to quantify the

deposition rate of asphaltenes upon addition of different precipitants. The accumulation of asphaltene deposits inside the capillary tube was confirmed and quantified by measuring the pressure difference between inlet and outlet.

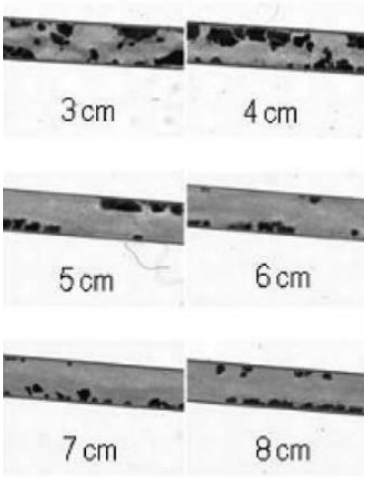

Figure 3-3. Deposition decrease as a function of the distance from the capillary entracnce at the end of the experiment with a flow rate of 10 µL min-1 . Taken from Boek et al.[57]

While Wang et al. [24] used a stainless steel coiled capillary tube, studies with straight metal capillary [60,61] have also been used to estimate the deposit formation amount and distribution as a function of the pressure drop across the capillary tube. Flow loop apparatus have also been used to study asphaltene precipitation[62,63] and deposition based on the pressure drop measurement across an in-line filter.

Some studies present evidence that the precipitant amount increases asphaltene deposition.[60] Using a fixed flow rate and changing the heptane ratios up to 50 vol. % for two petroleum fluids very little deposition took place when small precipitant amounts were used, but when the precipitant amount was increased

more deposition occurred.[60] For larger metal pipes (24 mm diameter) both decreasing flow rate and increasing asphaltene content increased deposition.[64] Some studies suggest that low flow rates and high asphaltene content enhance deposition.[25] Efforts to rescale raw pressure drop data failed to fully collapse the data.[60] Moreover, there is disagreement regarding the uniformity of deposition along the axial direction in a pipe. Evidence has been presented to suggest that deposition is uniform throughout a given length of pipe[24] and that it occurs mainly near the pipe inlet.[60]

More recently, Lawal et al.[65] reported experimental results obtained by examining asphaltene deposition in a glass microcapillary pipet, in an attempt to represent asphaltene deposition in reservoir pores. Also, Lin et al. [66] have shown significant progress in the development of micro-fluidic devices to probe asphaltene deposition in a porous medium. Their current work includes the fabrication of a high pressure and high temperature cell, to extend the investigation to more realistic conditions commonly found in oil reservoirs.

3.2.2. Organic solid deposition cell (OSDC)

Currently, the only commercial technology available to determine asphaltene deposition at high pressure, high temperature and under a turbulent flow regime was described in its initial stage by Zougari et al.[67] Further improvements were presented by Akbarzadeh et al.[68] In this device the live oil sample is held in the annulus formed between two concentric cylinders. Turbulence of the fluid is induced by rotating the inner cylinder while the outer cylinder remains static. This

configuration is known as a Taylor-Couette flow device. The pressure inside the device is maintained below the asphaltene onset pressure (AOP) and above the bubble pressure of the mixture. This allows asphaltene to precipitate and deposit on the surface of the cylinders. At the end of the experiment the liquid is evacuated and the deposited material is quantified and analyzed. The main improvement achieved with the recent version of this technique over its previous one is that it allows a continuous input of fresh oil sample, which is particularly necessary for crude oils with very low asphaltene content. This is because during pressure depletion, only a fraction of the asphaltenes in solution precipitate and only a small fraction of the amount that precipitates deposits on the surface. Thus, experiments that were previously operated in batch mode limit the volume of crude oil, which in turn, reduces the amount of asphaltene deposited. The low asphaltene content present in some reservoir fluids would not be sufficient to provide enough deposit for analysis within a reasonable experimental error.

3.2.3. Limitations of the Asphaltene Deposition Existing Techniques

Some of the limitations associated with existing testing techniques for asphaltene deposition evaluation are: [12]

- Amount of sample required for the test
- Adequate temperature control to ensure well defined thermal conditions
- High pressure and high temperature adaptability to mimic reservoir conditions

- Accuracy and precision of detection technique to generate reproducible and reliable data

- Ability to test different surface types and roughness to test actual pipeline materials and new surface materials and coatings

Chapter 4

Asphaltene Inhibitors Evaluation

4.1. Materials

Experiments were conducted with crude oil S from the Middle East that was decanted and centrifuged to remove aqueous phase and suspended particles. The properties for this crude oil have been reported elsewhere,[69] and are listed in Table 3-1. The commercial asphaltene dispersants 8, 9 and 15 were used to treat the crude oil samples. All reagents used for the experiments were a high performance liquid chromatography (HPLC) grade and were procured from Sigma Aldrich.

Asphaltene deposition studies experiments with model oil were conducted to establish the new system operation conditions. Model oil A was prepared by dissolving asphaltenes in toluene.

Crude oil A from the Gulf of Mexico (GOM) with an asphaltene concentration of 14 wt. % was used for the asphaltene extraction procedure. In order to extract

asphaltenes, crude oil was first dissolved in toluene with the ratio of 5 g of crude oil per 100 mL of toluene. A hot plate at 90 °C and ultrasonic bath at 40 kHz were repeatedly used to make sure all crude oil was dissolved in toluene. Then, the solution was centrifuged at 5000 rpm for 15 min to remove undissolved crude oil from it. The supernatant fluid was then mixed with n-pentane at the ratio of 1:5 in volume (1 mL of supernatant fluid to 5 mL of n-pentane). The mixture was allowed to rest for 1 hour and then centrifuged for 15 min at 5000 rpm to separate the precipitated asphaltene fraction. Then, the supernatant fluid was withdrawn, and the sediment was washed using pure n-pentane to remove non-asphaltenic materials from the deposited asphaltenes. The addition of n-pentane to the sediment and subsequent centrifugation and removal of supernatant fluid were repeated 3 times until no color was observed in the supernatant liquid. The deposited asphaltenes in the centrifuge tubes were dissolved in toluene, and the solution was heated in a beaker to remove all liquid from the solid asphaltenes. It should be noted that this procedure is a quick method for extracting asphaltenes from crude oil but it is not a technique for quantifying the asphaltene content of the oil. Also, n-pentane was used here because higher amounts of asphaltenes can be extracted using n-pentane compared to other n-alkanes.[29]

4.1.1. Model Oil Preparation

Model oil A with asphaltene concentration of 1 wt. % was prepared by adding the proper amount of toluene to the asphaltenes to reach the desired asphaltene concentration. The asphaltenes re-dissolution was performed at 90 °C

and using ultrasonication at 40 kHz for 30 min. To ensure there were no undissolved asphaltene particles in the mixture, the solution was centrifuged at 85000 rpm for 20 min. No sediment was observed after centrifugation.

The selection of 1 wt. % for the concentration of asphaltenes in the model oil A was somewhat arbitrary but represents a low asphaltene concentration, which is typical in light crude oils with propensity to show asphaltene deposition problems in the field.

4.2. Commercial Asphaltene Dispersants Effect on Asphaltene Aggregation

Figure 4-1 (a) portrays the HPHT test results for crude oil A and Figure 4-1 (b) shows direct spectroscopy results for crude oil S at ambient conditions. Crude oils S and A were obtained from two different wells from the same oil field. To induce the precipitation of asphaltenes at ambient conditions, n-heptane was added to crude oil S, which provides the driving force for asphaltene precipitation, instead of the pressure depletion used in the HPHT experiments. Figure 4-1 (b) shows light intensity vs. crude oil and heptane vol. %. According to this Figure the light intensity increases as the crude oil is diluted by the addition of the precipitant; this is the same trend observed in the case of HPHT experiments. In the latter case the dilution of the sample is caused by the expansion of the fluid. In either case, when the driving force for precipitation is high enough, the formation of asphaltene aggregates causes a drop on transmittance of light. In the case of the experiment performed at ambient

pressure, according to Figure 4-1 (b), the addition of n-heptane first dilutes the asphaltenes in solution (0 – 40% n-heptane), then causing their precipitation (40-60% n-heptane) and finally, as more n-heptane is added, both the asphaltene aggregates and the components from the oil remaining in solution are diluted, increasing the transmittance of the light (> 60% n-heptane). From Figure 4-1 (a) and (b) it is clear that results from direct spectroscopy performed at ambient conditions and results obtained at high pressure and temperature show similar trends before and at the onset of asphaltene precipitation. However, unlike the experiments conducted at ambient pressure in which the effect of dilution is observed after the onset of precipitation, in the case of high pressure and temperature experiments, the bubble point is attained and the composition of the remaining liquid is no longer constant at low enough pressure. In fact, as the pressure decreases below the bubble point the concentration of asphaltene increases in the liquid phase, which in turn reduces the transmittance of light. Moreover, due to the formation of gas bubbles the transmittance recorded below the bubble point pressure does not correspond to that of the liquid phase.

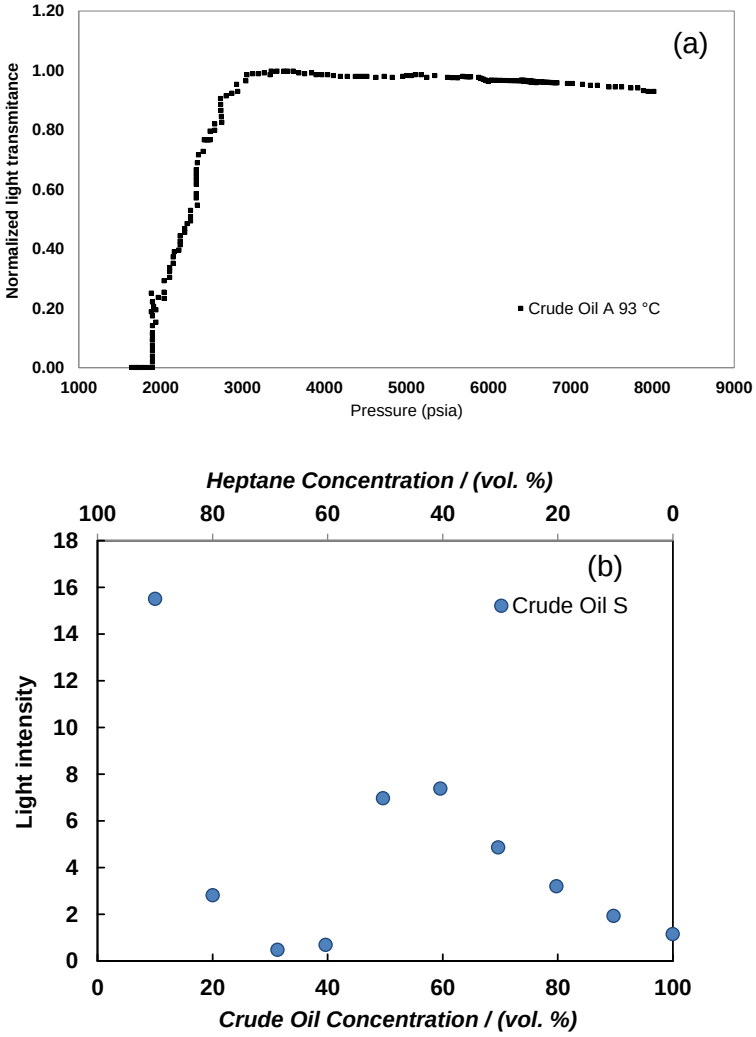

Figure 4-1. Results for crude oil A and crude oil S (a) Results for AOP measurement using NIR and HPM for Crude Oil A at 93°C (b) Direct spectroscopy results for Crude Oil S diluted with n-heptane and aged for 1 h at 25˚C

The results of experiments at ambient pressure can be presented in a different way, by: (1) removing the effect of dilution, (2) normalizing the light intensity data and (3) plotting the results in a logarithmic scale. Figure 4-2 displays the same experimental results as Figure 4-1 (b), after the implementation of the three transformation steps. The logarithmic scale is needed to enhance the changes

of the light intensity for high concentrations of n-heptane. Also, with this post-processing technique, the onset of asphaltene precipitation can be readily obtained as the point where the first deviation from the horizontal line is observed. Therefore, this technique to process and report the experimental data will be used throughout the rest of the document for direct spectroscopy results and interpretation, which will be discussed in detail in Section 4.2.3.

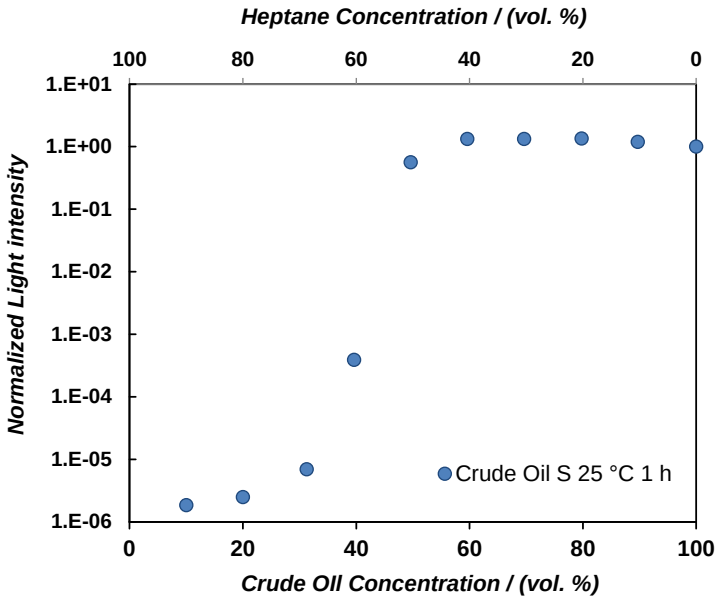

Figure 4-2. Direct spectroscopy results for crude oil S diluted with n-heptane and aged for 1 h at 25˚C. Normalized light intensity and corrected to remove the effect of dilution.

4.2.1. Asphaltene Dispersion Test - ADT Experimental Procedure and Results

Crude oil S was treated with dispersants 8, 9 and 15. Different chemical dosages were tested. For dispersant 8, 9 and 15, 70 ppm and 500 ppm were prepared and analyzed. All solutions were prepared by diluting a concentrated solution, e.g. 3,000 ppm, of the corresponding dispersant in crude oil. The

homogenization of the sample was achieved in a close beaker for a period of one hour using a magnetic stirrer. A crude oil S sample without dispersant was used as control. 250 μL of the different treated and untreated crude oil were placed in graduated centrifuge tubes and mixed with 9.75 mL of n-heptane.

Finally, the samples were left undisturbed for a specific period of time (also known as aging time) and the amount of sediment obtained was recorded in mL at the end of the experiment. The experiments were repeated for aging times of 1 hour, 24 hours and 1 week

When no sediments were observed the data entry was recorded as "clear" and when precipitation was observed but was not measurable the data entry was recorded as "trace".[13] The criterion for evaluation of the performance of dispersants using the Asphaltene Dispersion Test (ADT) consists of comparing the amount of sediment obtained in mL for the different chemicals and dosages with respect to the blank or untreated oil, which was the mixture of crude oil and n-heptane without the addition of the dispersant.

The results are shown in Figure 4-3 and the volume of sediment obtained in the different cases is presented in Table 4-1. Since the criterion for evaluating the performance of the chemical based on the ADT test consisted on comparing the volumes of sediment obtained with the presence of the inhibitor at the different dosages against the control. The lower the amount of sediment collected the more efficient the dispersion of asphaltenes.

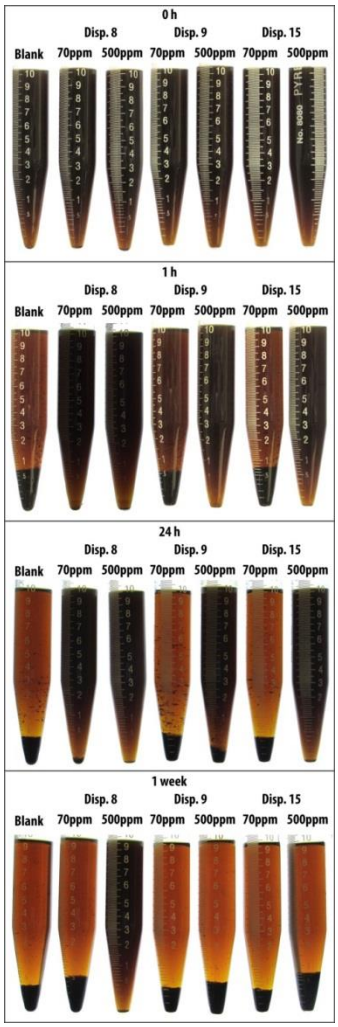

Figure 4-3. ADT Test results for Crude oil S treated with dispersants 8, 9 and 15 at 70 ppm and 500 ppm for aging times of 0 hours, 1 hour, 24 hours and 1 week.

After 24 hours, only the samples treated with dispersant 8 and 15 at 500 ppm did not show any sediment. After 1 hour the untreated crude oil presented sediments and at longer times the sediment levels decreased as reported in Table 4-1. According to the results presented in Section 4.2, the amount of precipitated asphaltene actually increases with longer aging times. Therefore the reduction of

the level of sediment could be the result of sediment compaction over time. The same observation is applicable to dispersant 9 and 15 at 70 ppm.

In addition, based on direct spectroscopy results from section 4.2 for a treated system when the heptane concentration approaches 100%, the result approached that of a stable solution. Since the ADT test requires large amounts of heptane, the result obtained from ADT could be misleading because the dispersant cannot be tested at the heptane concentration that causes the highest precipitation of asphaltene and/or the largest asphaltene aggregates.

Table 4-1. ADT for Crude Oil S treated with dispersants 8, 9 and 15 at 70 and 500 ppm.

Sample	Dosage (ppm)	0 hour (ml)	1 hour (ml)	24 hour (ml)	6 days (ml)
Crude Oil S	NA	Clear	0.7	0.4	0.3
Disp 8	70	Clear	Clear	Trace	0.5
	500	Clear	Clear	Clear	Clear
Disp 9	70	Clear	0.5	0.4	0.3
	500	Clear	Clear	0.2	0.5
Disp 15	70	Clear	0.7	0.4	0.3
	500	Clear	Clear	Clear	0.7

4.2.2. Direct method Experimental Procedure

Blends of crude oil S with and without dispersants were prepared following the same procedure explained in section 4.2.1. Blends of different ratios of crude oil

(with and without dispersant) and n-heptane were prepared ranging from 0 to 90 volume% of n-heptane. The test tubes were shaken by hand and the blends were transferred to 10-mm path length quartz cuvettes that were then tightly closed. To maintain a homogeneous temperature the samples were kept inside a Jeio Tech oven model OV-11/12 at a specific temperature; 25˚C and 70˚C were used in this work. The samples were allowed to rest undisturbed for the specified aging time. In this case, the aging time is the period of time allotted between sample preparation and the measurement of NIR transmittance. The masses of added oil and precipitant were measured and the actual volumes were back calculated assuming an ideal solution. Then, the NIR transmittance was measured using a Shimadzu UV-Vis-NIR spectrophotometer Model UV-3600 equipped with a "TC1 Temperature Controller" and a "t2×2 Dual Temperature-Controlled Cuvette Holder" provided by Quantum Northwest. Inside this chamber the samples were mixed at 1,000 rpm with a magnetic stirrer that was placed inside the cuvette. During the measurement the samples were stirred to prevent the sedimentation of any asphaltene aggregates that could be present in the system. This technique provided a more reproducible result, compared to static unstirred systems in which the sedimentation of the asphaltene aggregates can affect the results.

The transmittance values were measured for wavelengths ranging between 1,000 and 1,300 nm. It was found that different wavelengths in this rage can be used to detect the onset of precipitation as long as the signal is not saturated. At wavelengths below 1,000 nm, it was not possible to obtain a measurement due to the signal saturation. The relative masses of oil and precipitant present in each

blend were measured and the corresponding volumes were back-calculated using the density of the components, assuming an ideal mixing. The transmittance values of the different samples were corrected by subtracting the transmittance of n-heptane and then the effect of dilution was mathematically removed. Details for the correction of the dilution effect have been explained by Tavakkoli et al.[29] The corrected transmittance values were then normalized using the transmittance of the crude oil as the reference. The normalized values are usually plotted as a function of the volume fraction of n-heptane or crude oil. However, the same results can also be presented in terms of light intensity (i.e. light transmittance) instead of transmittance, which is how the results are usually reported by direct spectroscopy. In the latter case, asphaltene precipitation was determined by the decrease in the normalized light intensity caused by asphaltene aggregates that block the path of light. The first deviation from the linear trend indicated the precipitation of asphaltenes. The normalized light intensity as a function of the volume fraction of crude oil and n-heptane can be plotted.

After NIR transmittance values were recorded, the samples were observed under a microscope AmScope model B340, coupled with a MU300 microscope digital camera operating at a combined magnification of 400x to confirm the existence of asphaltene aggregates.

4.2.3. Direct Method Results

Direct spectroscopy was also used as an alternative approach to the ADT to assess the performance of asphaltene dispersants. Figure 4-4 shows the average for

three different data sets obtained for crude oil S at 25˚C for an aging time of 1 hour. Error bars are included for each point as evidence that the data trend was very similar in repeated experiments. The experiments' average was plotted in each figure and the Average Standard Deviation (ASD) was reported in the figure caption indicating the data repeatability.

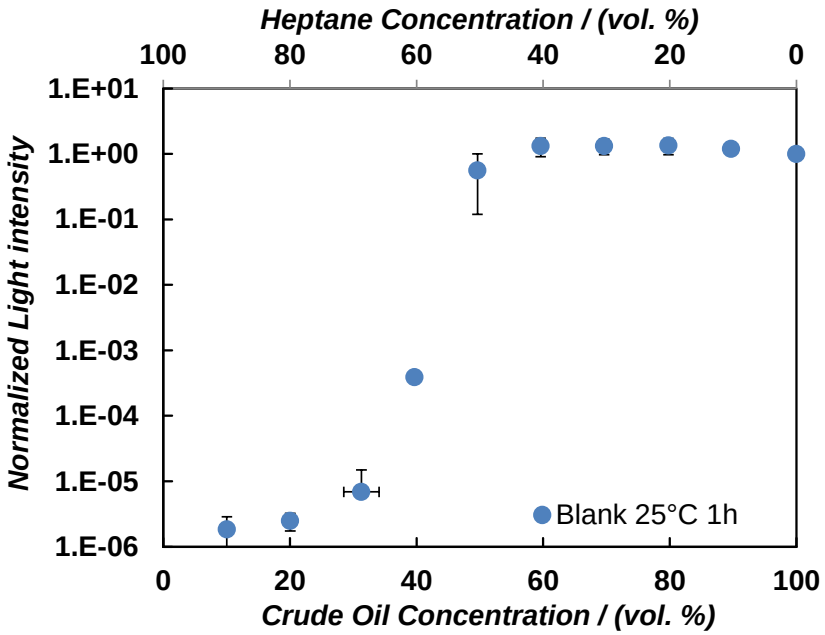

Figure 4-4. Direct method results for the crude oil S diluted with n-heptane and aged for 1 h at 25˚C. The ASD is 6.03%

4.2.3.1. Effectiveness of Commercial Asphaltene Dispersants

In order to identify the most effective dispersant for crude oil S, different aliquots of this crude were treated with a dosage of 70 ppm of dispersants 8, 9 and 15 and aged for 1 hour at 25°C. Lower dosages of inhibitors are desirable for field applications in an attempt to minimize the treatment cost. The results are presented

in Figure 4-5. This Figure has two sections: the first section Figure 4-5 (a) is a nearly horizontal line at low precipitant amounts and high crude oil vol. %. Then, there is a second section in Figure 4-5 (b) at high precipitant amounts and low crude oil vol. % where the light intensity values deviate from the horizontal trend. The point at which this deviation occurs represents the volume fraction of precipitant required for the detection of asphaltene precipitation. Once the detection of asphaltene precipitation is reached, the light intensity decreases as more precipitant is added to the system. The continuous drop of the light intensity at higher amounts of precipitant is an indication of the increase in the number and size of asphaltene aggregates.

Figure 4-5 (b) shows a progressive light intensity reduction for the blank after the detection of asphaltene precipitation. When the system was treated with dispersant 8 the response was similar with respect to the blank until the detection of asphaltene precipitation. Once this point was reached the light intensity dropped at a slower rate than the blank as observed in Figure 4-5 (b) indicating a slower precipitation and aggregation rates under the effect of dispersant 8. Then, when the heptane concentration approached 100 vol. % the treated system showed a second inflection point at 70 vol. % where the light intensity increased again approaching the horizontal base line that represents a stable solution indicating the presence of less and/or smaller aggregates. Addition of n-heptane has two effects on the precipitation of asphaltenes: on one hand it dilutes the asphaltene content and therefore its light intensity decreases, even when there is no precipitation (at volume fractions below 50 vol. %); on the other hand, it slows down the

precipitation and aggregation kinetics. The first effect can be accounted for by multiplying the measured transmittance by the dilution factor. In the presence of a dispersant the kinetics of asphaltene precipitation and aggregation is further reduced and, therefore, the light intensity is greater than the blank, for a given aging time. As the aging time increases the light intensity usually drops and the difference between treated and untreated samples is reduced. This will be discussed in detail in section 4.2.3.3.

Figure 4-5 (c) shows the results for the three dispersants and the control (i.e. blank). As expected, the light intensity after the detection of asphaltene precipitation was higher for the treated systems than the blank. The bigger the difference among the treated and untreated system after the detection of asphaltene precipitation, the better the dispersant performance since less and/or smaller particles are being formed. Under these conditions dispersant 8 was the most effective chemical according to Figure 4-5 (c). Dispersant 15 exhibited the weakest dispersive effect among the three samples.

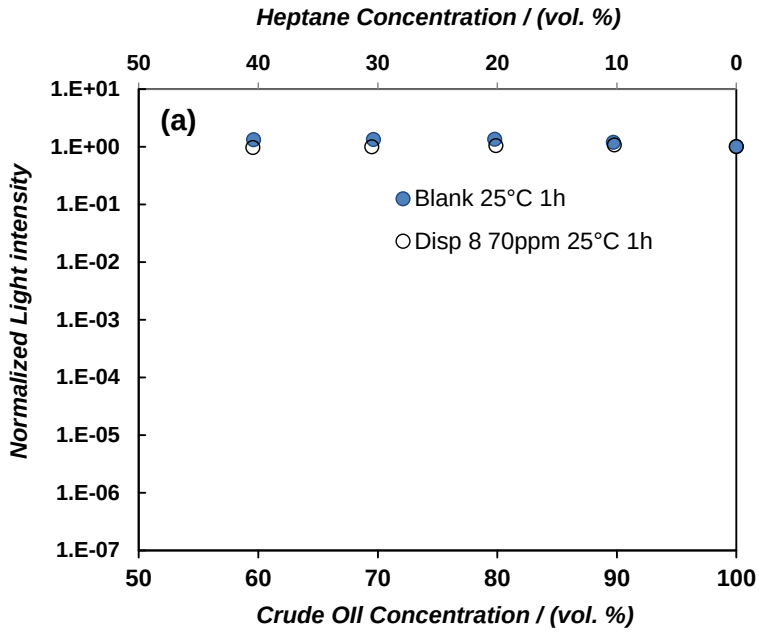
Heptane Concentration / (vol. %)
50
40
30
20
10
0
(a)
Blank 25°C 1h
Disp 8 70ppm 25°C 1h
Normalized Light intensity
1.E+01
1.E+00
1.E-01
1.E-02
1.E-03
1.E-04
1.E-05
1.E-06
1.E-07
50
60
70
80
90
100
Crude Oil Concentration / (vol. %)

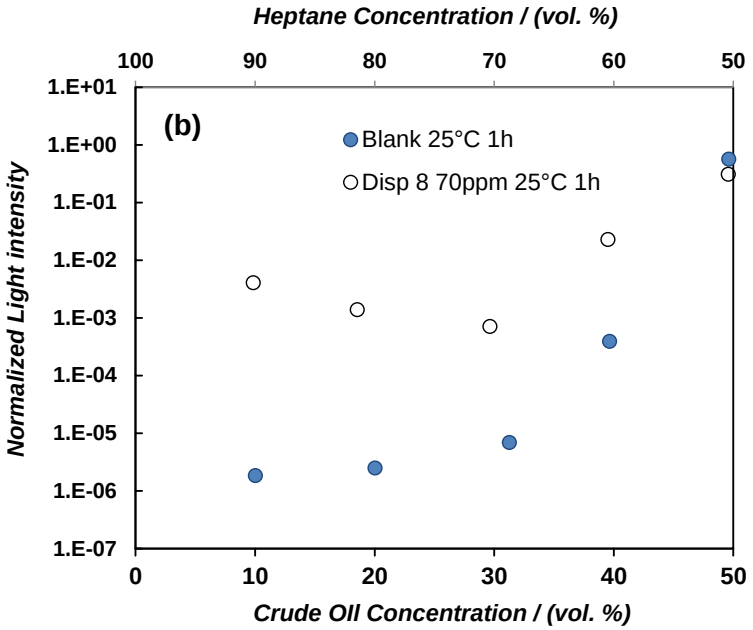
Heptane Concentration / (vol. %)
100
90
80
70
60
50
(b)
Blank 25°C 1h
Disp 8 70ppm 25°C 1h
Normalized Light intensity
1.E+01
1.E+00
1.E-01
1.E-02
1.E-03
1.E-04
1.E-05
1.E-06
1.E-07
0
10
20
30
40
50
Crude Oil Concentration / (vol. %)

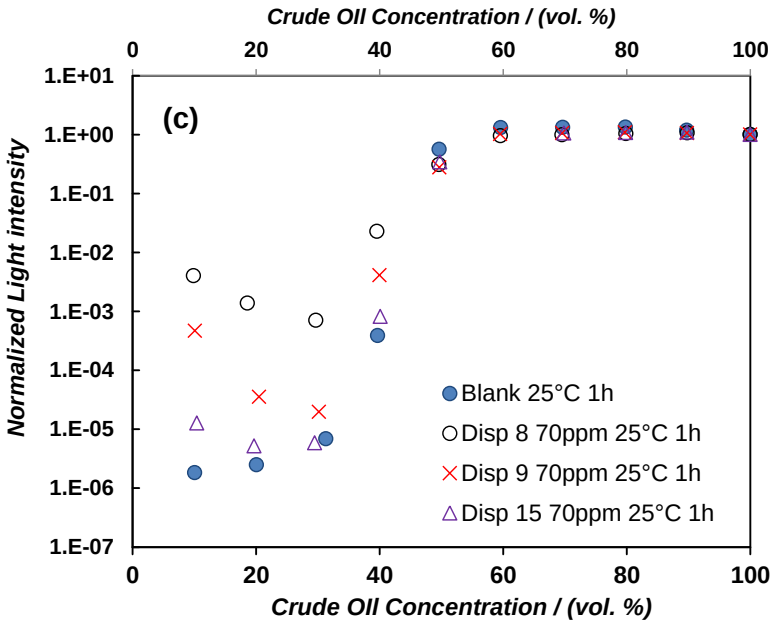

Figure 4-5. Direct method results for the crude oil S with a 70-ppm dosage of different commercial dispersants, after mixing with heptane and aging for 1 h at 25˚C. (a) Dispersant 8 vs. Blank, 50-100 vol.% n-heptane, (b) Dispersant 8 vs Blank, 0-50 vol.% n-heptane. (c) Dispersants 8, 9 and 15 vs. Blank. The ASD are 6.03%, 5.31%, 6.82% and 3.21% for the blank, dispersant 8, 9 and 15, respectively.

To enhance the accuracy in the determination of the volume percent of n-heptane at the detection of asphaltene precipitation, more samples were prepared near this point. Then, for the first section and the beginning of the second section regression curves were fitted. The detection of asphaltene precipitation is calculated as the intersection between these two lines. Figure 4-6 shows an example for one test of dispersant 9 at 70 ppm after 1-hour aging time. The detection of asphaltene precipitation was calculated for repeated experiments and the average is reported in terms of the precipitant vol. %.

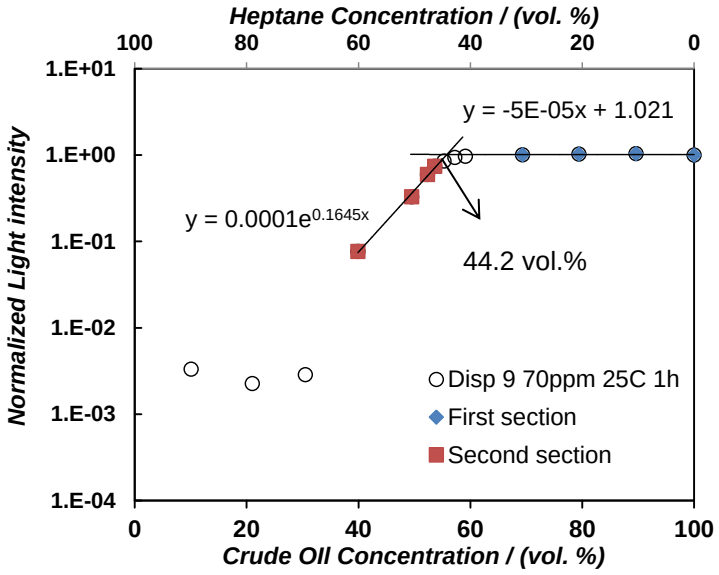

Figure 4-6. Results of the direct method for the crude oil S, mixed with a 70-ppm dosage of dispersant 9, diluted with n-heptane and aged for 1 h at 25°C.

Table 4-2 shows the treated and untreated crude oil S detection of asphaltene precipitation after 1-hour aging time. At these conditions, according to the results obtained using the direct method, there is a slight change in the onset of asphaltene precipitation caused by the addition of the dispersant.

Table 4-2. Detection of asphaltene precipitation of crude oil S with a 70-ppm dosage of different commercial dispersants, after mixing with heptane and aging for 1 h at 25°C

Sample	Detection of asphaltene precipitation (n – heptane vol. %)
Blank	48.8 ± 2.6
Dispersant 8	46.2 ± 3.0
Dispersant 9	45.5 ± 1.9
Dispersant 15	47.6 ± 1.3

In order to understand the asphaltene-dispersant interactions, additional effects have been studied.

4.2.3.2. Effect of Dosage

To understand the effect of the dosage on dispersants 8, 9 and 15, studies with different concentrations of each dispersant at 70 ppm and 500 ppm were performed, at 25˚C and 1 hour of aging time. The results are shown in Figure 4-7.

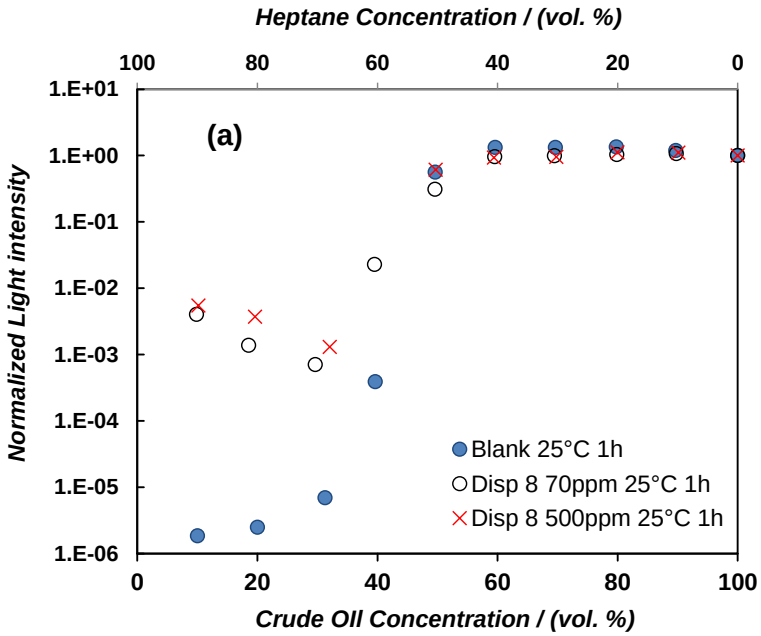

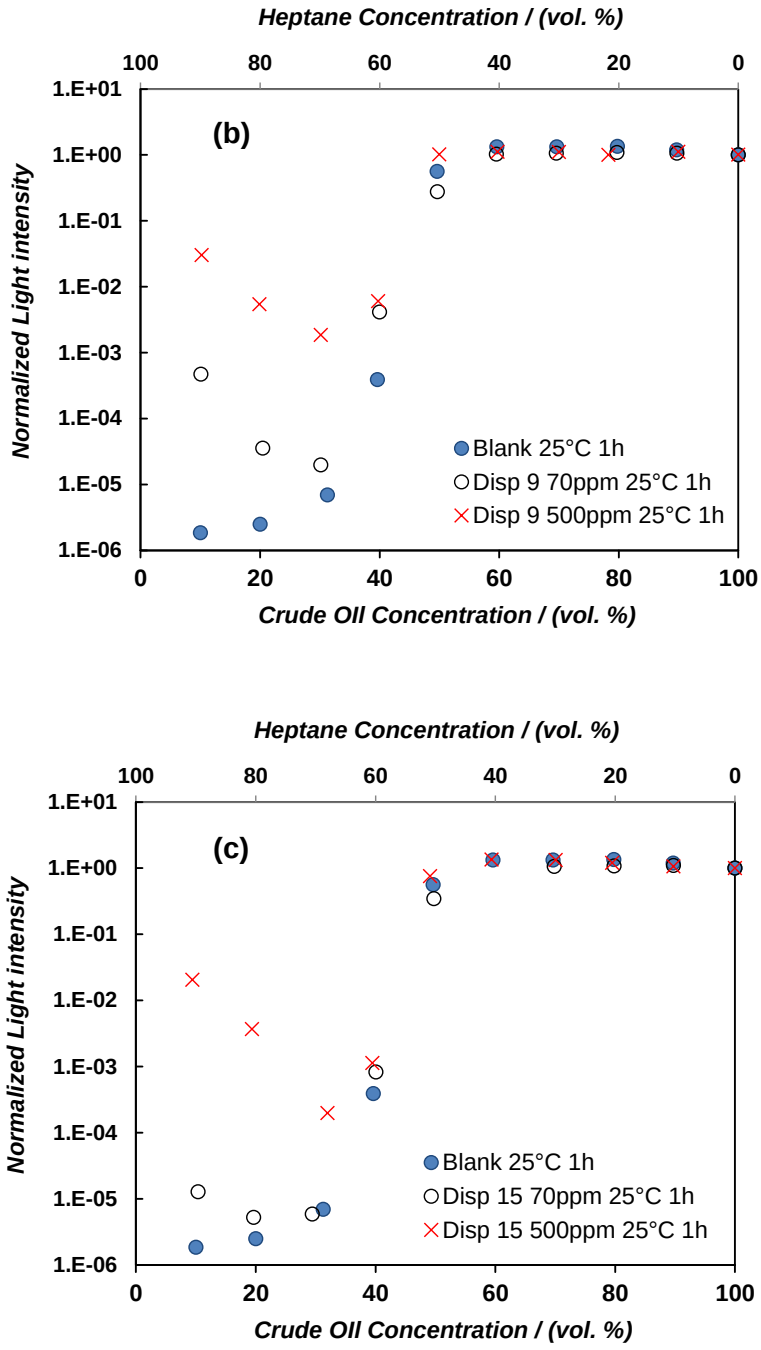

Figure 4-7. Direct method results for crude oil S with *(a)* Dispersant 8 *(b)* Dispersant 9 (c) Dispersant 15 at different dosages, after mixing with n-heptane and aging for 1 h at 25˚C. The ASD are 6.03%, 5.31%, 6.82%, 3.21%, for the blank, dispersant 8, 9 and 15 at 70 ppm and 2.43%, 0.502%, 0.017% for dispersant 8, 9 and 15 at 500 ppm, respectively.

As observed in Figure 4-7 (a), dispersant 8 had similar results at the two different dosages. The benefit was marginally better for the higher dispersant dosage and only for heptane concentrations of 70 vol. % and 80 vol. %. This is in agreement with the idea that there is an optimal concentration of asphaltene dispersant and, depending on the system characteristics, the size of the asphaltene aggregates remains nearly constant even if more dispersant is added.[16]. As discussed in section 4.2.1 the ADT results after 1 hour for dispersant 8 at 500 ppm did not show significant sedimentation. However, from direct spectroscopy results it was observed that there was asphaltene precipitation and aggregation in the presence of dispersant 8 at 500 ppm after one hour, but it was slower compared to the aggregation observed in the blank.

On the other hand, Figure 4-7 (b) and (c) showed for dispersants 9 and 15 that increasing the dispersant dosage causes a reduction in asphaltene aggregation and consequently, an increase on light transmittance. At 500 ppm both dispersants 9 and 15 significantly reduced asphaltene aggregation.

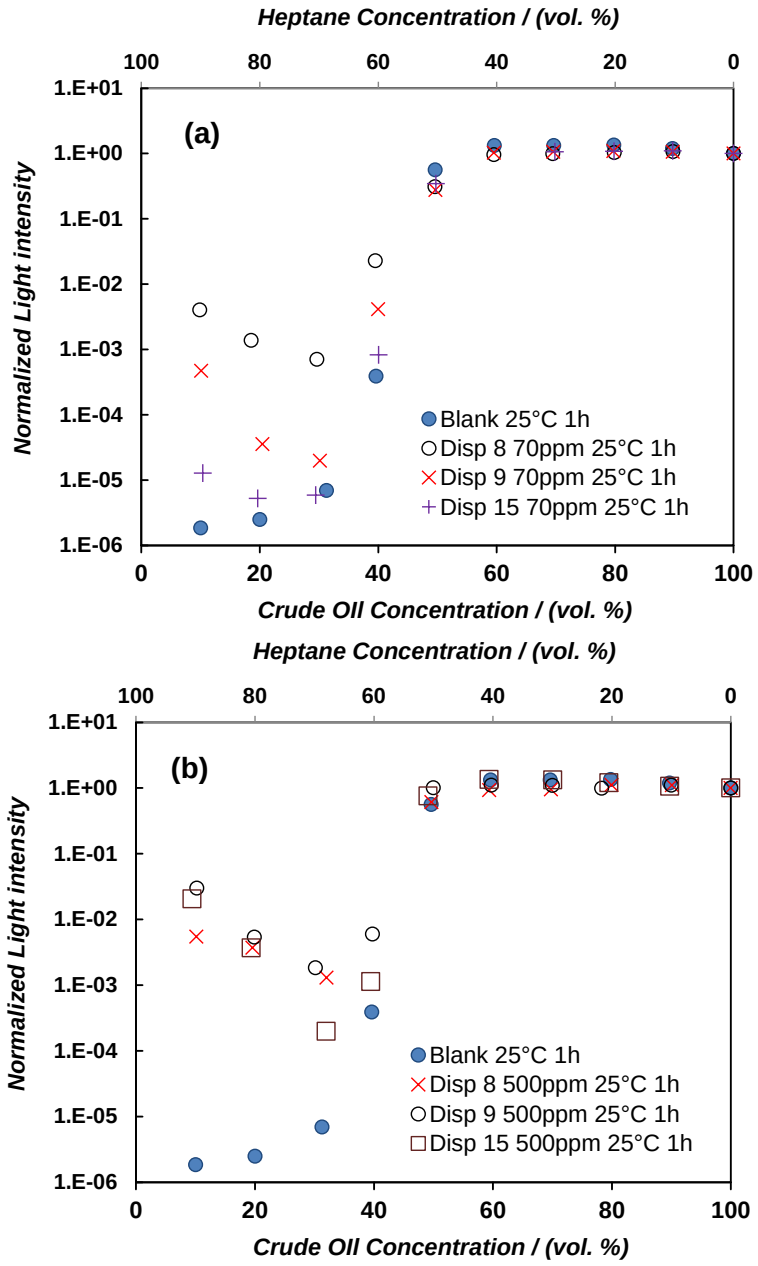

Figure 4-8. Results of the direct method for the crude oil S with (a) Dispersant 8, 9 and 15 at 70 ppm (b) Dispersant 8,9, and 15 at 500 ppm, after mixing with heptane and aging for 1 h at 25˚C. The ASD are 6.03%, 5.31 %, 6.82%, 3.21%, for the blank, dispersant 8, 9 and 15 at 70 ppm, and 2.43%, 2.62%, 0.46%, for dispersant 8, 9 and 15 at 500 ppm, respectively.

According to Figure 4-8 (b), when Crude oil S was treated with dispersants 8, 9 and 15 at 500 ppm all samples showed almost the same level of performance. However, at the lower dosage of 70 ppm, inhibitor 8 outranked inhibitors 9 and 15. Therefore, according to this technique inhibitor 8 at 70 ppm seems a reasonable choice. Treating a well at high dosages is not economically viable as was previously discussed in Section 2.2.

Table 4-3. Detection of asphaltene precipitation of crude oil S with 500 ppm dosage of different commercial dispersants, after mixing with heptane and aging for 1 h at 25˚C .

Sample	Detection of asphaltene precipitation (n – heptane vol. %)
Blank	48.8 ± 2.6
Dispersant 8	49.5 ± 1.9
Dispersant 9	50.1 ± 1.8
Dispersant 15	49.8 ± 2.1

Table 4-3 shows the onset of asphaltene precipitation for treated crude oil S with 500 ppm of dispersant after 1 hour aging time. The blank used for comparison is crude oil with no inhibitor. The onset of asphaltene precipitation shows a slight change upon addition of the asphaltene dispersant.

4.2.3.3. Effect of Aging Time

As it was previously defined in section 4.2.2., the aging time corresponds to the time elapsed between sample preparation and the measurement of light

intensity. The effect of aging time on the detection of asphaltene precipitation and aggregation phenomena, as well as on the performance of different dispersants, is considered in this section. Figure 4-9 shows direct method results for the blank and crude oil S treated with dispersants 8 and 9 at 70 ppm for different aging times, namely 1 hour, 24 hours and 2 weeks. Dispersant 15 was not evaluated because it did not show a significant effect after 1 hour at 70 ppm as discussed in section 4.2.3.2. Figure 4-9 shows that for all aging times dispersant 8 at 70 ppm performed better than dispersant 9. In addition, for all the treated and untreated systems the asphaltene aggregation was a function of time and increased as time passed. Thus, with time asphaltenes that precipitated and were detected after one hour continue to aggregate even in the presence of asphaltene dispersants. This suggests that dispersants slow the aggregation process down, but they cannot prevent the occurrence of asphaltene precipitation or aggregation.

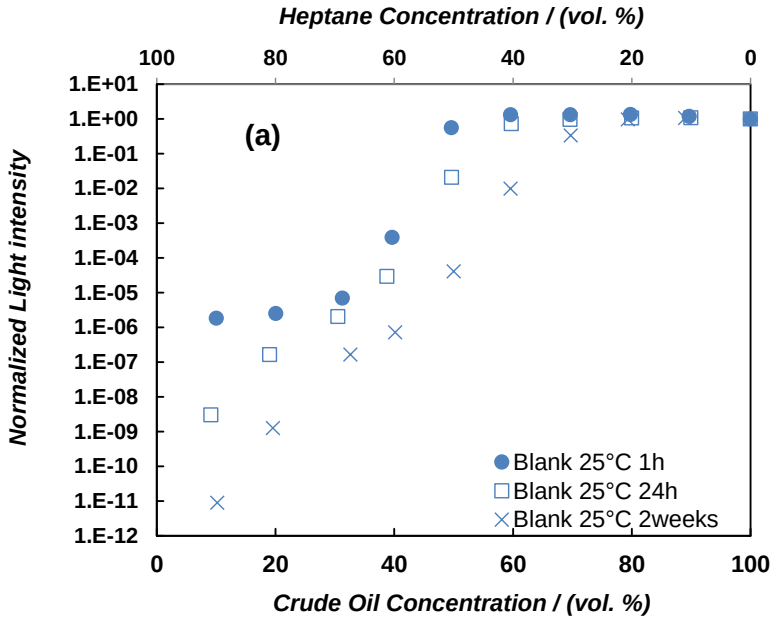

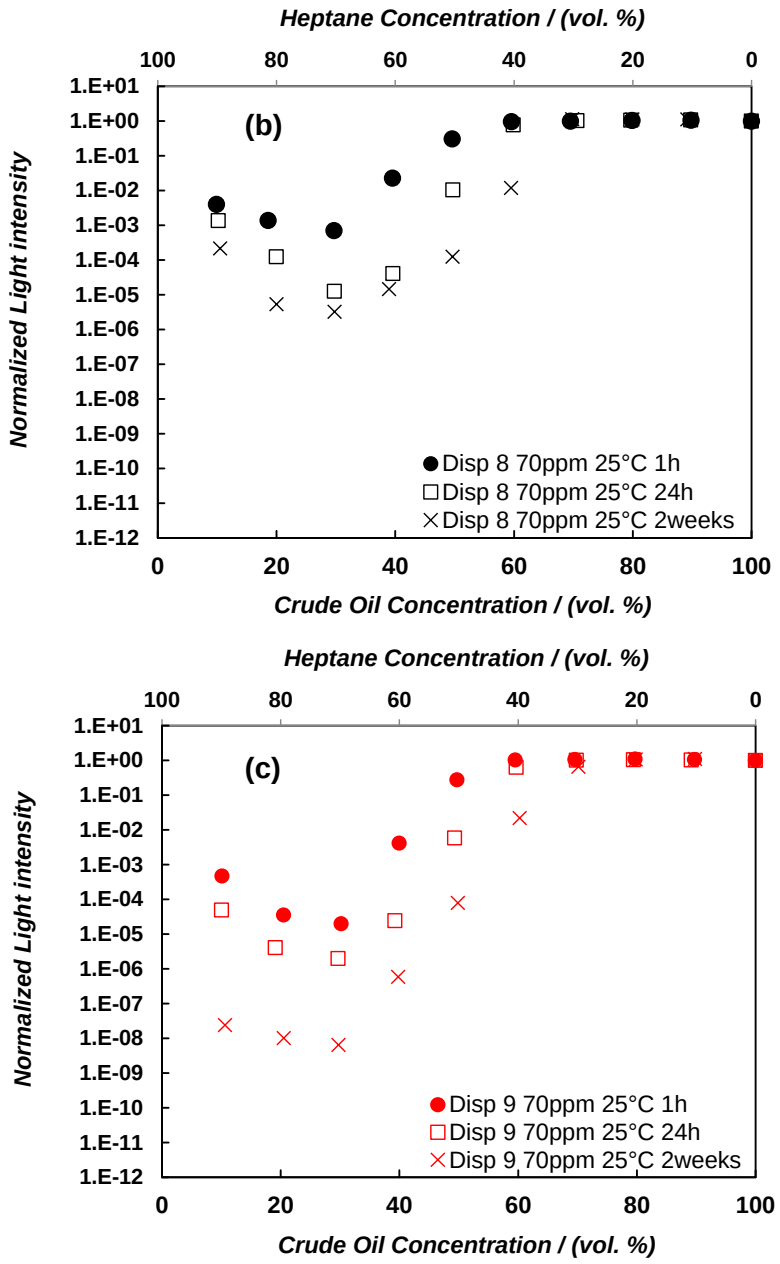

Figure 4-9. Results of the direct method for the crude oil S with (a) Blank (b) Dispersant 8 at 70 ppm (c) Dispersant 9 at 70 ppm, after mixing with heptane and aging for 1 h, 24 h and 2 weeks at 25˚C. The ASD are 6.03%, 5.57% and 2.55% for the blank at 1 h, 24 h and 2 weeks, respectively. 5.31 %, 2.18%, 1.79% for dispersant 8 at 1 h, 24 h and 2 weeks, respectively. 6.82%, 3.20%, 4.27% for dispersant 9 at 1 h, 24 h and 2 weeks respectively

The detection of asphaltene precipitation was determined in the manner explained in section 4.2.3.1 and results are reported in Table 4-4. The volume of n-heptane needed to induce the precipitation of asphaltene significantly decreased when the aging time increased from one hour to two weeks. According to Table 4-4, the effect of aging time is much more prominent than the effect of asphaltene dispersant. For both untreated and treated systems the longer the aging time the less precipitant is needed to induce the asphaltene precipitation.

Table 4-4. Detection of asphaltene precipitation of crude oil S threated with different commercial dispersants at 70 ppm, after mixing with heptane and aging for 1 h, 24 h and 2 weeks at 25˚C

Sample	Asphaltene Onset Concentration (AOC) (n – heptane vol. %)			
	1 h	24 h	2 weeks	ΔAOC_{max}
Blank	48.8 ± 2.6	42.4 ± 1.6	28.3 ± 0.6	20.5
Disp 8	46.2 ± 3.0	41.3 ± 1.3	29.7 ± 0.1	16.5
Disp 9	45.5 ± 1.9	39.5 ± 0.9	32.4 ± 1.7	13.1

Some studies have reported that a logarithmic relation between aging time and detection of asphaltene precipitation exists.[70] A similar trend was found in this work. Figure 4-10 shows the onset of asphaltene precipitation for different asphaltene dispersants as a function of time.

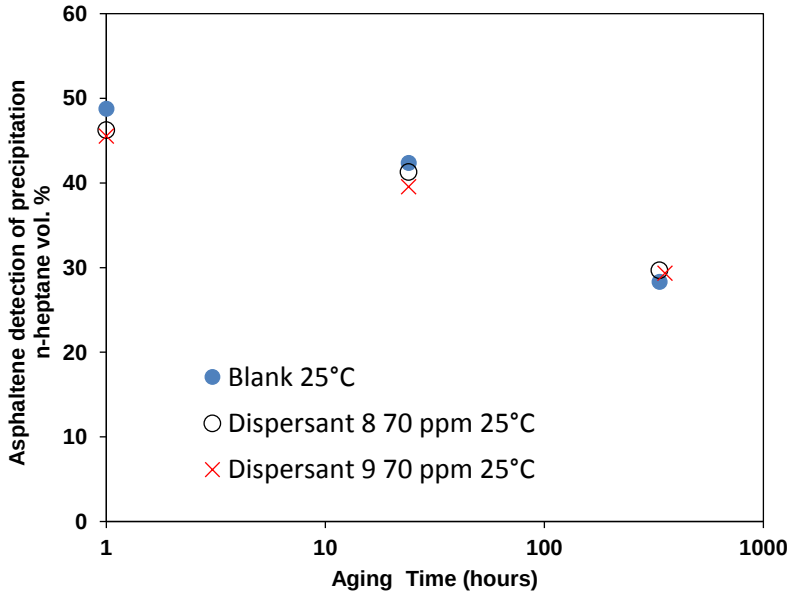

Figure 4-10. Detection of asphaltene precipitation after 1 hour, 24 hours and 2 weeks aging time for crude oil S without adding dispersants, and with dispersants 8 and 9 at 70 ppm dosage. Time axis in log scale.

4.2.3.4. Effect of Temperature

In order to study the temperature effect on the performance of different dispersants, experiments at 25°C and 70°C were conducted for 24 hours. The same dosages used to evaluate the dispersant effect on section 4.2.3.1 were evaluated.

It is important to consider the effect of temperature on the thermodynamic properties of the system. Temperature variations induce changes in asphaltene solubility, crude oil density and viscosity, since all these properties are temperature dependent. The solubility of asphaltenes in oil usually increases with increasing temperature, because at this phase boundary temperature, the entropy gain from

mixing just overcomes the enthalpically-favored phase splitting.[71] Moreover, due to the polydisperse nature of the asphaltenes, the asphaltene fraction that precipitates at high temperature may differ from that which precipitates at lower temperature. Different asphaltene fractions have different properties such as density and diffusion rate. Only the more unstable asphaltenes precipitate at a higher temperature. At the same time, at higher temperature the crude oil density and viscosity decrease and less dense and less viscous blends can accelerate the aggregation process. Thus, the effect of temperature on the performance of a given dispersant can be very significant.

Figure 4-11 shows the effect of temperature on blends of oil and n-heptane with and without dispersants. The system appeared to be more stable at 70°C than at 25°C without the presence of the dispersant. Figure 4-11 (a) shows the crude oil or blank results and it can be observed that the aggregation and precipitation rates were lower when increasing temperature. At higher temperature, the crude oil was a better solvent for the asphaltenes and more precipitant was needed to induce precipitation. Figure 4-11 (b) and Figure 4-11 (c) show the results for dispersant 8 at 70 ppm and 500 ppm at 25°C and 70°C after 24 hour aging time, respectively. It can be observed for dispersant 8 at 70 ppm that the difference with respect to the blank was higher at 25°C than at 70°C. In other words, at 25°C dispersant 8 reduced the aggregation more effectively than at 70°C. Therefore, when the temperature increased the dispersant performance decreased.

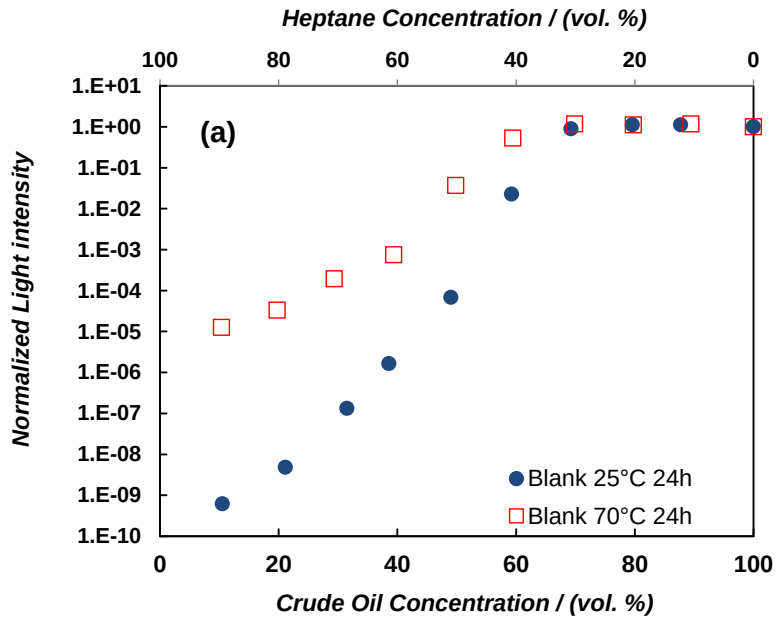
Heptane Concentration / (vol. %)
100
80
60
40
20
0
1.E+01
1.E+00
1.E-01
1.E-02
1.E-03
1.E-04
1.E-05
1.E-06
1.E-07
1.E-08
1.E-09
1.E-10
(a)
Normalized Light intensity
Blank 25°C 24h
Blank 70°C 24h
0
20
40
60
80
100
Crude Oil Concentration / (vol. %)

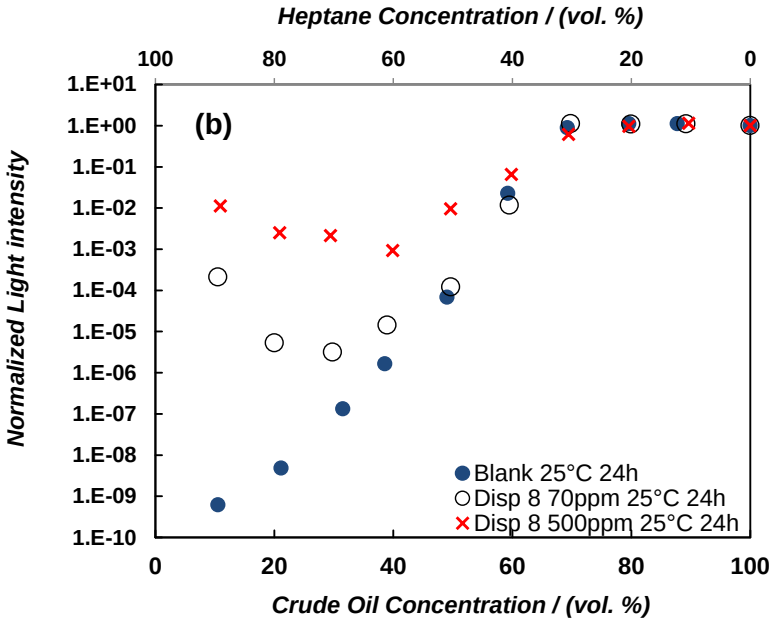
Heptane Concentration / (vol. %)
100
80
60
40
20
0
1.E+01
1.E+00
1.E-01
1.E-02
1.E-03
1.E-04
1.E-05
1.E-06
1.E-07
1.E-08
1.E-09
1.E-10
(b)
Normalized Light intensity
Blank 25°C 24h
Disp 8 70ppm 25°C 24h
Disp 8 500ppm 25°C 24h
0
20
40
60
80
100
Crude Oil Concentration / (vol. %)

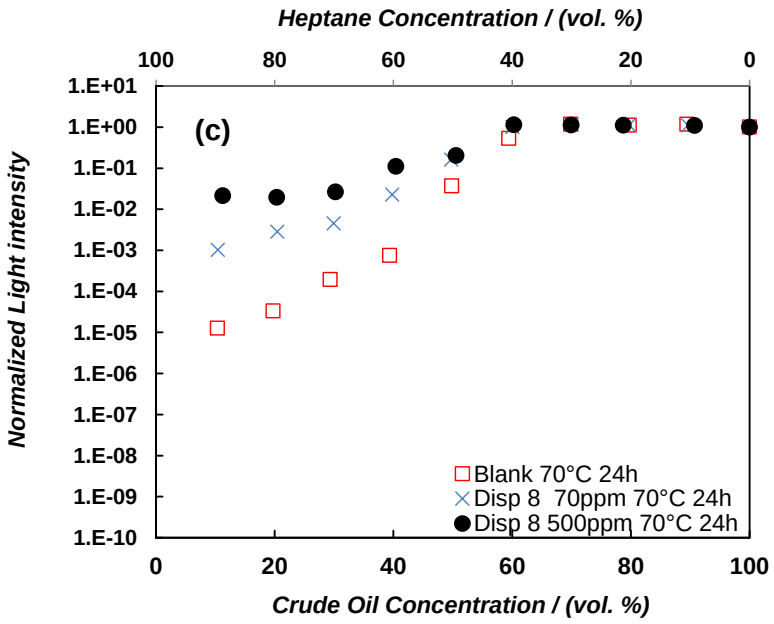

Figure 4-11. Results of the direct method for the crude oil S for (a) Blank (b) Dispersant 8 at 70 and 500 ppm (c) Dispersant 8 at 70 and 500 ppm, after mixing with heptane for 24 hours at 25˚C and 70˚C. The ASD are 2.44%, 3.34%, 4.68%, 6.20%, 5.98%, 1.89% for blank 25˚C, blank 70˚C, dispersant 8 at 70 ppm and 500 ppm at 25˚C, dispersant 8 at 70 ppm and 500 ppm at 70˚C, respectively.

Analogous experiments were conducted with dispersant 9 at 70 ppm, 25˚C and 70˚C for 24 hours. Figure 4-12 (a) shows the effect of dispersant 9 at 25˚C. As previously discussed in sections 4.2.3.1 and 4.2.3.2, dispersant 9 did not disperse asphaltene aggregates as efficiently as dispersant 8 under the same conditions, but it had still some effect over this system. Figure 4-12 (b) shows results for dispersant 9 when temperature changes from 25˚C to 70˚C. Similarly to the previous observation, dispersant 9 performance decreased with increasing temperature.

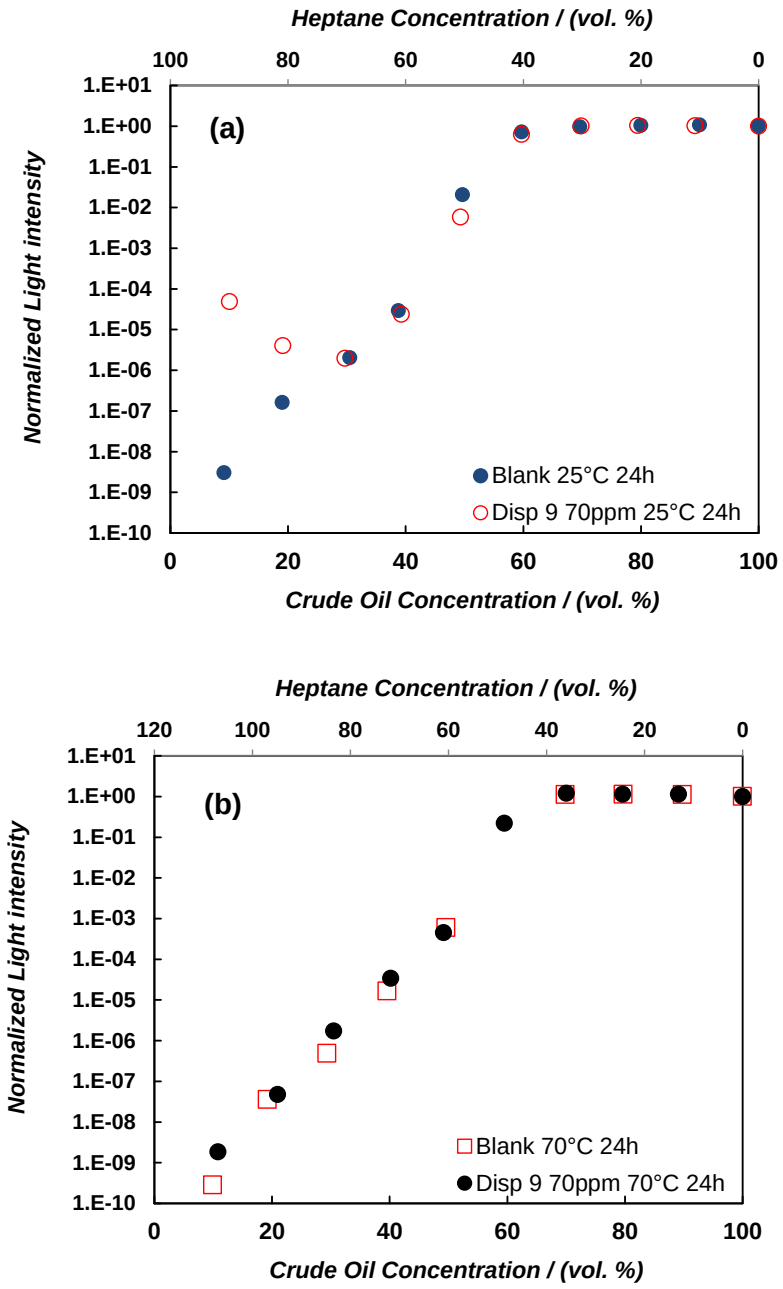

Figure 4-12. Results of the direct method for the crude oil S for (a) Dispersant 9 at 25°C (b) Dispersant 9 at 70°C, after mixing with heptane for 24 hours. The ASD are 5.57%, 3.20% for the blank and Dispersant 9 at 25°C and 3.34%, 2.11% for the blank and Dispersant 9 at 70°C, respectively.

Dispersant 15 was also studied at 70 ppm and 70°C and the results showed poor performance. As previously discussed in sections 4.2.3.1 and 4.2.3.2, dispersant 15 did not disperse asphaltenes even at room temperature condition.

4.2.3.5. Definition of Dispersive Performance

To facilitate the ranking of different asphaltene dispersants, dispersive performance efficiency is introduced. The efficiency is calculated as follows:

P： Dispersive Performance Efficiency

$$\mathbf{DPE} = \mathbf{100} * \left(\mathbf{1} - \frac{\mathbf{A^{Disp.Formulation}}}{\mathbf{A^{Blank}}}\right)$$

Equation 4-1. Dispersive Performance Efficiency

$$\mathbf{A} = \int_{\mathbf{10}}^{\mathbf{100}} -\mathbf{Log_{10}(Light\ intensity)dC_{crude\ oil}}$$

Equation 4-2. Area under the curve calculation for DPE

Where A^{Blank} represents the area between the curve for the blank and the base horizontal line and $A^{Disp.Formulation}$ represents the area between the curve for the treated system and the horizontal base line. The areas can be estimated using a numerical recipe, such as the trapezoidal rule. Table 4-5 presents the results for dispersants 8, 9 and 15 at different concentrations, temperatures and aging time

conditions. Since dispersive performance for crude oil S without dispersant is zero for all temperatures and aging time conditions, this is not presented in Table 4-5.

Table 4-5. Dispersive performance efficiencies for Dispersants 8, 9 and 15 at different dosages, temperatures and aging time conditions. Efficiency and Maximum efficiency* reported.

Dispersive Performance - Efficiency (%) – Max. Efficiency (%)*					
		1 hour	24 hours		2 weeks
Sample	Dosage (ppm)	25 °C	25 °C	70 °C	25 °C
Disp 8	70	46.9 - 58.3*	28.8 - 66.0*	42.2 - 43.0*	15.8 - 50.0*
	500	51.5 - 61.1*	58.0 - 77.6*	62.1 - 65.3*	NA
Disp 9	70	22.7 - 41.9*	14.3 - 49.3*	8.9 - 10.4*	7.1 - 30.8*
	500	54.1 - 72.9*	--	---	---
Disp 15	70	7.3 - 15.4*	---	---	---
	500	40.3 - 68.8*	---	---	---

Table 4-5 summarizes the dispersant efficiencies and restates the trends that have been already discussed in this document. As previously discussed in section 4.2.3.1, for experiments performed at 70 ppm, 25˚C and 1 hour aging time dispersant 8 was the most effective dispersant (DPE = 46.9%), followed by dispersant 9 (DPE = 22.7%) and dispersant 15 (DPE = 7.3%). These results indicate that under these conditions dispersant 8 reduced the aggregation rate more effectively than the other two dispersants.

At all aging times evaluated, i.e. 1 hour, 24 hour and 2 weeks, at 70 ppm and 25˚C, dispersant 8 performed better than dispersant 9. After 24 hours, dispersant 8 (DPE = 28.8%) is more effective than dispersant 9 (DPE = 14.3%). Then, after two

weeks dispersants 8 (DPE = 15.8%) has better efficiency than dispersant 9 (DPE = 7.1%) as well.

When dispersants concentration increased to 500 ppm, at 25˚C and after 1 hour aging time, dispersant 9 had the best dispersive performance (DPE = 54.1%), followed by dispersant 8 (DPE = 51.5%) and dispersant 15 (DPE = 40.3%). In addition, as discussed in section 4.2.3.2, dispersant 8 at 70 ppm, 25˚C and after 1 hour aging time had dispersive performance (DPE = 46.9%) very close to the dispersants at high concentration.

According to the previous discussion in section 4.2.3.4 when the temperature is kept constant and the dispersant dosage was increased, a higher dispersive effect was observed. For dispersant 8 after 24 hours aging time, the efficiency rose from 28.8 % to 58% at 25˚C and from 42.2% to 62.1% at 70˚C when the dosage was increased from 70 ppm to 500 ppm, respectively. At 70˚C, 70 ppm and 24 hours aging time dispersant 8 (42.2%) once again was more effective than dispersant 9 (8.9%).

High reservoir temperatures can severely impact the dispersant performance efficiency. Chemical additives need to be designed to work at a wide range of temperature conditions. The dispersive performance efficiency should be calculated against a blank that is held at the same temperature and aging time conditions.

Dispersant 8 showed the best performance at almost all conditions, followed by dispersant 9 and dispersant 15. This trend only changed at 500 ppm dosage,

25˚C, 1 hour aging time where dispersant 9 was slightly more efficient than dispersant 8.

In the case of chemical additives that perform as asphaltene dispersants, it is important to take into consideration - as Vargas has reported[10] - that reducing the particle size or in other words, enhancing the dispersion effect, might not necessarily help in preventing deposition.

4.3. Effect of Commercial Asphaltene Dispersants on the Precipitation of Asphaltene

Commercial chemical additives have been tested to study their effect on asphaltene precipitation and aggregation phenomena using two different techniques: “Indirect method” and “Direct spectroscopy”.

4.3.1. Experimental Procedure for the Indirect Method

Crude oil S was treated with dispersants 8 and 9. Different chemical dosages were tested. For dispersant 8, dosages of 70 and 500 ppm were used, whereas for dispersant 9, samples containing 70, 500 and 2,000 ppm were prepared and analyzed. Crude oil and all solutions were prepared as explained in section 4.2.1.

Blends of different ratios of crude oil (with and without dispersant) and n-heptane were prepared as explained in section 4.2.2 In this case the aging time is the period of time allotted between sample preparation and centrifugation. Afterwards, the samples were centrifuged at a g-force of 12,000 for 15 min to

remove particles of 100 nm and above. An aliquot of the supernatant liquid was withdrawn and diluted with toluene, which stabilizes the asphaltenes that remained in solution avoiding further aggregation. Dilution with toluene reduces the absorbance and prevents any saturation, so Beer-Lambert's law is applicable. Then, light absorbance was measured at wavelengths ranging from 700 nm to 1,300 nm with a Shimadzu UV-Vis-NIR spectrophotometer Model UV-3600, using air as the blank. The cuvettes used for the spectroscopic measurements are made of quartz with a path length of 10 mm. The measured values were corrected to account for the effect of dilution and then normalized using the absorbance of the crude oil sample, in the same way as was explained in section 4.2.2.

The normalized values are finally plotted as a function of volume fraction of n-heptane or crude oil. The first deviation from linear trend indicates the precipitation of asphaltenes. The same results can also be presented in terms of light intensity (i.e. light transmittance) instead of absorbance, which is how the results are usually reported by indirect method. In the latter case, asphaltene precipitation is determined by the decrease in the absorbance caused by asphaltene aggregates that block the path of light. The normalized light intensity as a function of the volume fraction of crude oil and n-heptane can be plotted.

4.3.2. Indirect Method Results

In Section 4.2.3 it was noted that the addition of dispersants caused a slight shift in the onset of precipitation. To further investigate the underlying cause for this shift, the indirect method was employed to detect the onset of asphaltene

precipitation. In Section 3.1.4, the features of the Indirect Method were briefly described. This method is much more sensitive for detection of the onset of asphaltene precipitation. The indirect method was used to study the effect of dispersants 8 and 9 on asphaltene precipitation from crude oil S diluted with n-heptane and aged for 24 hours at 25˚C. The results are usually reported as absorbance vs. precipitant vol. % as observed in Figure 4-13 (a), (b) and (c) where the decrease in the absorbance value with respect to the horizontal line is an indication of the precipitation of asphaltenes.[29] The drop in absorbance is proportional to the amount of asphaltene precipitated from the oil. Figure 4-13 (a) and (b) show the absorbance values for dispersant 8 and 9 respectively at 70 ppm, 25˚C and 24 hours aging time. In both cases with and without the addition of a dispersant the results are almost identical at the different concentrations of added n-heptane. For dispersant 8, according to Figure 4-13 (c), even when the dosage is increased to 500 ppm the results do not change significantly. Therefore, the presence of an asphaltene dispersant did neither affect the onset of precipitation nor the amount of precipitated asphaltenes.

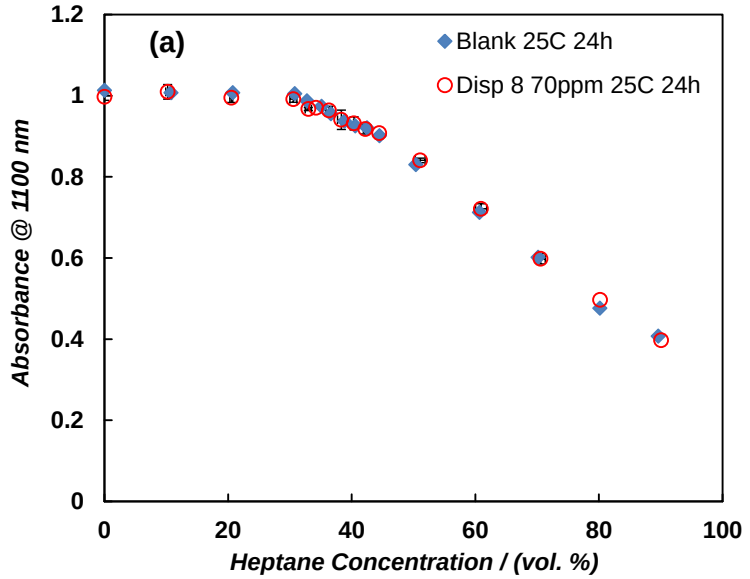
(a)
Blank 25C 24h
Disp 8 70ppm 25C 24h
Absorbance @ 1100 nm
Heptane Concentration / (vol. %)
0
0.2
0.4
0.6
0.8
1
1.2
0
20
40
60
80
100

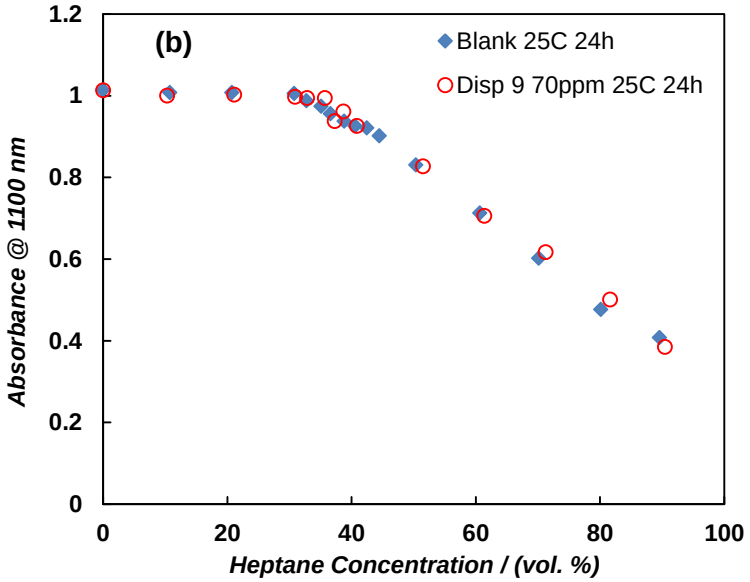
(b)
Blank 25C 24h
Disp 9 70ppm 25C 24h
Absorbance @ 1100 nm
Heptane Concentration / (vol. %)
0
0.2
0.4
0.6
0.8
1
1.2
0
20
40
60
80
100

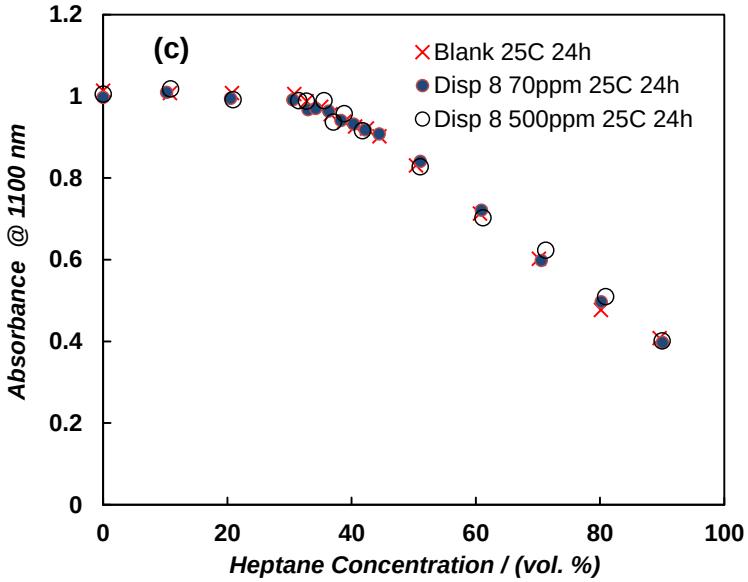

Figure 4-13. Indirect method results for crude oil S with (a) Dispersant 8 and (b) Dispersant 9 at 70 ppm dosage (c) Dispersant 8 at 70 ppm and 500 ppm, after mixing with heptane and aging for 24 h at 25˚C. The ASD are 2.15% for the blank, 1.51%, 1.4% and 1.0%, for dispersant 8 and dispersant 9 at 70 ppm, and dispersant 8 at 500 ppm respectively.

For consistency, results of the indirect method were also plotted as a function of the normalized light intensity vs. crude oil vol. % and heptane vol. %. Figure 4-14 (a), (b) and (c) presents the same results as Figure 4-14. In this case the light intensity increase with respect to the horizontal line is the indication of the asphaltene precipitation. The more asphaltenes are removed upon precipitation the higher the intensity of the light.

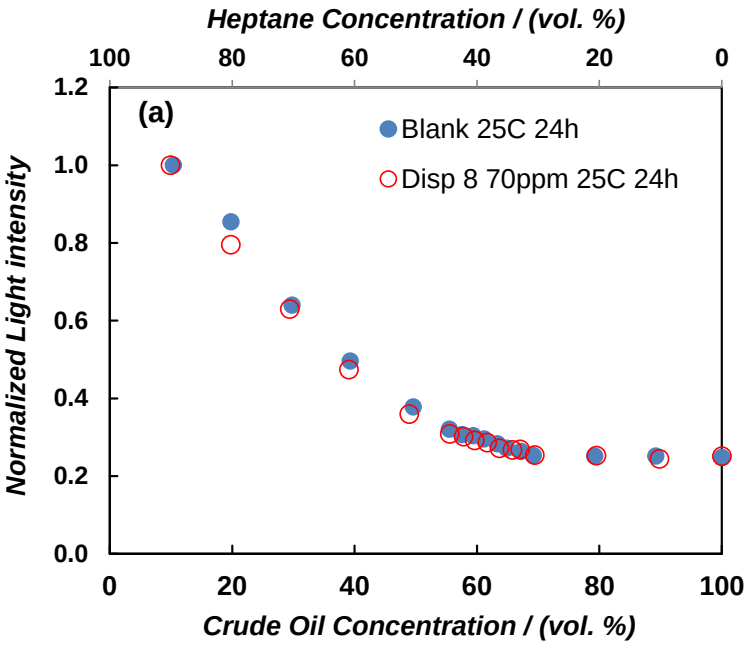
Heptane Concentration / (vol. %)
100
80
60
40
20
0
(a)
Blank 25C 24h
Disp 8 70ppm 25C 24h
Normalized Light intensity
1.2
1.0
0.8
0.6
0.4
0.2
0.0
0
20
40
60
80
100
Crude Oil Concentration / (vol. %)

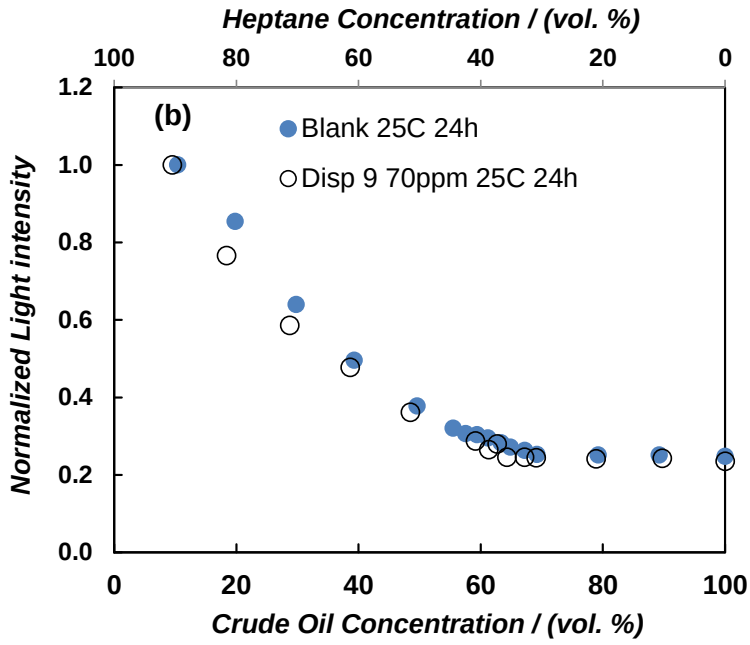
Heptane Concentration / (vol. %)
100
80
60
40
20
0
(b)
Blank 25C 24h
Disp 9 70ppm 25C 24h
Normalized Light intensity
1.2
1.0
0.8
0.6
0.4
0.2
0.0
0
20
40
60
80
100
Crude Oil Concentration / (vol. %)

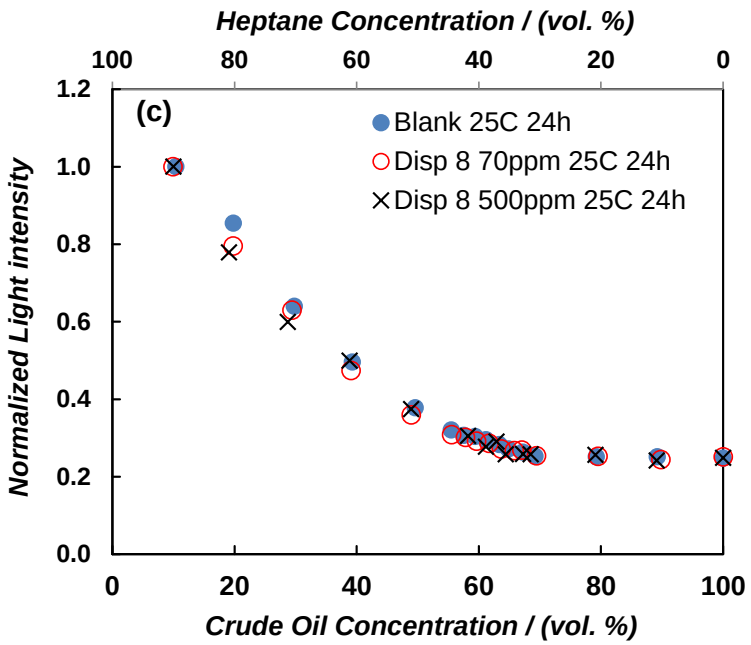

Figure 4-14. Indirect method results reported as normalized light intensity vs. crude oil vol. % and heptane vol. % for crude oil S with (a) Dispersant 8 at 70 ppm (b) Dispersant 9 at 70 ppm dosage (c) Dispersant 8 at 70 ppm and 500 ppm, after mixing with heptane and aging for 24 h at 25˚C. The ASD are 2.15% for the blank, 1.51%, 1.4% and 1.0% for dispersant 8 and dispersant 9 at 70 ppm and dispersant 8 at 500 ppm respectively.

After 24 hours of aging time Figure 4-14 shows a lower detection of asphaltene precipitation compared to the direct method results presented in Table 4-4 in section 4.2.3.3. This is an indication of the superior sensitivity of the indirect method [29] which allows for the detection of smaller particles.

Crude oil S was treated with 2000 ppm of dispersant 9, at 25˚C for 24 hours and was evaluated using direct and indirect methods. Similarly to the observation from the HPHT test, Figure 4-15 (a) shows the results for direct method and a shift in the detection of asphaltene precipitation for the treated system at ambient pressure. The detection of asphaltene precipitation increased from 22.4 to 28.8 n-

heptane vol. % when the concentration of inhibitor increased from 0 to 2,000 ppm. This could be misinterpreted to mean such as in the HPHT test that the dispersant seems to stabilize the crude oil, because there is a shift on the detection of asphaltene precipitation towards a larger precipitant amount. However, Figure 4-15 (b) shows the indirect method results, in which there was neither a change on the detection of asphaltene precipitation nor the amount of asphaltene precipitate observed.

To reconcile these results, one should look at the limitation of the techniques used. Once the asphaltenes start precipitating, the process leads to the formation of small particles in the order of 100 to 400 nm [29,72] that can further aggregate at later stages. The detection limit of the direct method is about 0.5 to 1 μm. [29] Thus, although the precipitated particles may already be present in the solution the onset of precipitation via direct method can only be detected when the asphaltene aggregates have grown to exceed the minimum detection limit. Since the aggregation rate is slowed down by the action of the dispersant, the particle size remains undetectable for a longer time or while larger amounts of asphaltene precipitant are added, which can give a false impression of increased stability. Because the indirect method is much more sensitive and particles as small as 100 nm can be detected, it is possible to differentiate the precipitation and aggregation steps. Consequently, the dispersants do not seem to affect the onset of asphaltene precipitation, only the rate of subsequent aggregation.

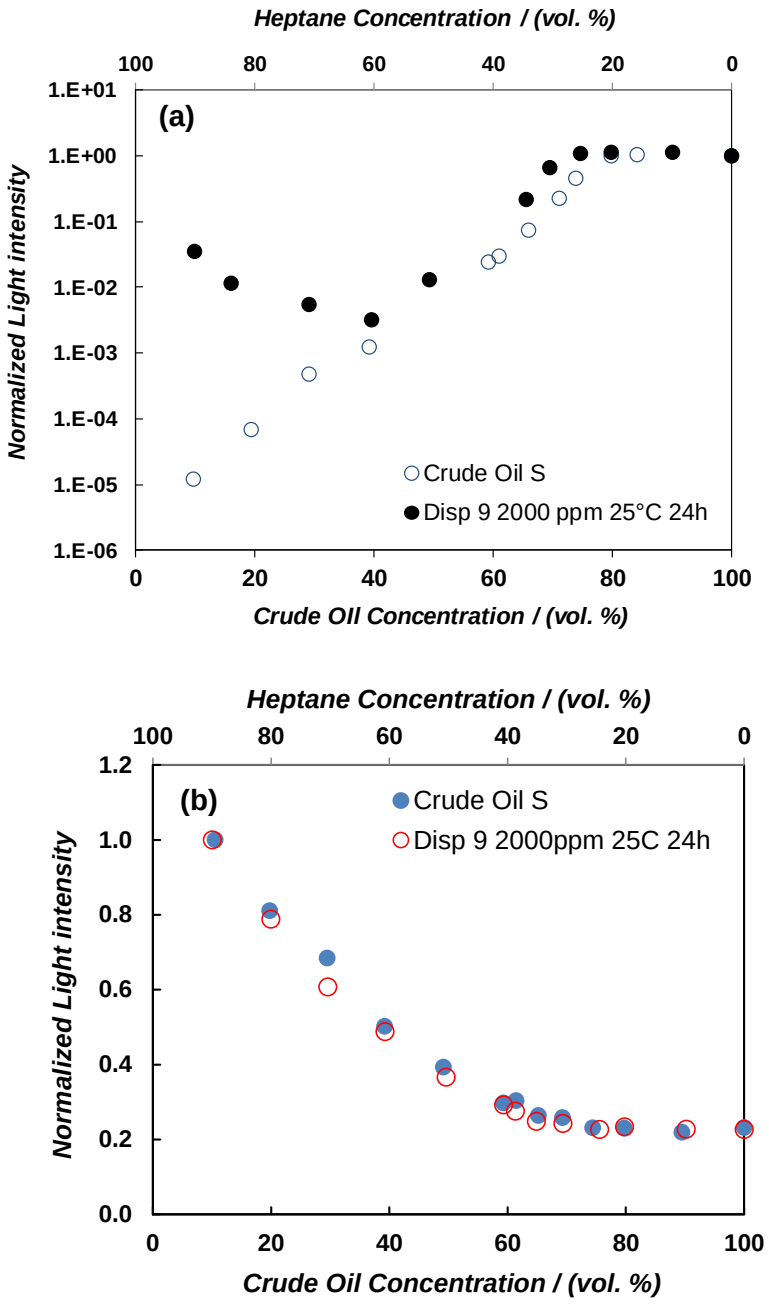

Figure 4-15. Results for crude oil S with a 2000-ppm dosage of dispersant 9, after mixing with heptane and aging for 24 h at 25˚C. (a) Direct method. The ASD are 3.17% and 3.27% for the blank and dispersant 9 respectively. (b) Indirect method. The ASD are 1.73% and 2.32% for the blank and dispersant 9 respectively.

4.4. Effect of Commercial Asphaltene Dispersants on the Deposition of Asphaltenes

4.4.1. Development of a New System for the Asphaltene Deposition Evaluation

A new system to study asphaltene deposition on metallic surfaces was developed. This new apparatus based on a column packed with carbon steel spheres and first depicted by Favero et al.,[73] offers advantages over the capillary systems. Unlike the system used by Favero et al[73] the version of the device developed in this work has the capability of assembling several column sections that can be analyzed independently. Currently, the device operates at ambient temperature and pressure and there is potential for the fabrication of a high- pressure system in the near future.

The system consists of a PTFE multi-section column system packed with carbon steel spheres to provide the surface area onto which asphaltenes can deposit. A schematic of the system is shown in Figure 4-20. The flow was driven through the column through PFA tubing, DuPont®-PFA Tubing Natural 1/16" OD x .020" ID, at a constant volume flow rate, using syringe pumps Harvard Apparatus Pump 11 Elite and Chemyx Fusion 100 and Hamilton Gastight Syringes (100 mL, 50 mL and 25 mL). The PFA tubing used to transport the oil and precipitant to the column inlet and from the outlet to the effluent collector was replaced with new tubing for each different experiment condition.

The experiments were performed at Reynolds number Re < 10 that for a packed bed corresponds to laminar flow regime.[74] The flow rate was established accordingly. The regime for flow through a packed bed is identified by the packed bed Reynolds number and was calculated using Equation 4-3. [74]

$$Re = \frac{x\, U_s\, \rho_f}{\mu\,(1-\varepsilon)}$$

Equation 4-3. Reynolds number for a packed bed

In Equation 4-3, x corresponds to the spherical equivalent particle diameter (m). The spherical equivalent particle diameter in this case is the diameter of the carbon steel spheres. U_s represents the superficial fluid velocity (m/s), ρ_f is the density of the fluid flowing through the packed bed (kg/m^3), μ is the viscosity of the fluid flowing through packed bed (Pa.s) and ε is the bed void fraction defined according to Equation 4-4. [74]

$$\varepsilon = \frac{Volume\ of\ voids\ in\ bed}{Total\ volume\ of\ bed\ (voids\ plus\ solids)}$$

Equation 4-4. Void fraction definition

The superficial velocity is the velocity of the fluid moving through the packed bed as if it was the only phase. The superficial velocity is calculated as the volumetric flow rate of the fluid moving through the packed bed (m^3/s) divided by the cross sectional area of the packed bed (m^2) as presented in Equation 4-5.

$$U_s = \frac{Q}{A}$$

Equation 4-5. Superficial velocity definition

For the study of transitional or turbulent flow regimes very large flow rates are required to increase the superficial velocity U_S. Due to the limitations of the system (i.e., pump total volume capacity, maximum flow rates and large amounts of oil and precipitant needed to reach large flow rates) it is not possible to achieve these conditions with the current system.

The experiments were conducted by charging one of the syringes with model oil A or crude oil S. Then, a second syringe was charged with the precipitant n-heptane. To prevent the pumps from damaging and guarantee enough sample in every syringe, the amount of precipitant and crude oil or model oil charged was greater than the total amount strictly required for the test. Before starting the test the air bubbles present in the samples charged in the syringes were removed by infusing liquid through the PFA tubing to a glass vial. The previous operation also worked to purge the flow lines from the syringe connection to the T-junction. Afterwards, the PEEK valves 2–Way 0.16 inch located between the syringe and the T-junction were closed and the PFA tubing was connected to the T-junction.

During some preliminary tests the presence of small bubbles was observed in the PFA tubing connecting from the mixing point to the column inlet. In an attempt to degas the liquids prior the beginning of the experiment the already charged syringes were immerse in the ultrasonic bath and the bubbles generated were

removed displacing the liquid contained in the syringe until no air bubbles were observed. However, this process was problematic for the oil samples due to foam formation that presented difficulties to completely remove the air present in the oil. This alternative did not significantly improve the reproducibility of the final results. Thus, it was not implemented as a standard procedure.

The next step consisted of programing the syringe pumps, according to the test conditions, opening the valves and starting the pumps simultaneously. At this point it was necessary to verify that all connections were properly adjusted and that no leaks on the T-Junction inside the ultrasonic bath were observed. In cases were leaks were observed, the test was stopped and restarted once the fitting connections were readjusted.

Both fluids were mixed in a T-junction, Tee Assembly Tefzel®-ETFE, for 1/16" OD, .020 thru hole, that was immerse in a Branson 1800 ultrasonic bath at 40 kHz, kept at constant temperature to promote well mixing. Then, the fluid flow from the bottom of the column (inlet) to the top (outlet) and the effluent was collected. The path between the T-junction (mixing point) and the column inlet was kept as short as possible (< 10 cm) to prevent asphaltene precipitation and / or asphaltene deposition to occur before the fluid entered the column, while still allowing maneuvering to assemble the system. And, the column was placed on top of the ultrasonic bath as shown in Figure 4-16.

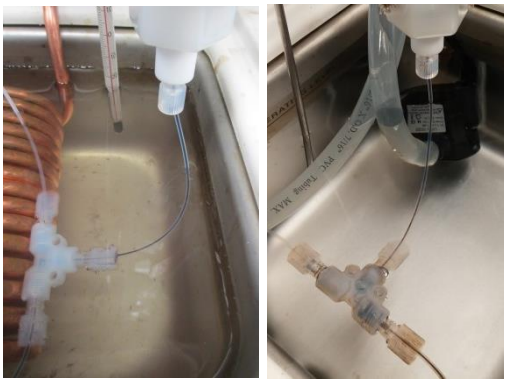

(**a**) (b**)**

Figure 4-16. Connection from Tee junction inmerse in the ultrasonic water bath to the inlet of the column. (a) Cooper cooling coil. (b) Water recirculation system.

As discussed in section 3.2.3, one of the limitations of techniques to evaluate asphaltene deposition is the lack of adequate temperature control to ensure well-defined thermal conditions. This difficulty was also faced in development of the system presented in this work. During the proof-of-concept tests it was observed that the ultrasonic bath temperature did not remain constant throughout all experiments due to the heating induced by the sonication. Thus, the temperature in the bath needed to be kept constant, which required the water inside the bath to be cooled down. A cooper cooling coil of 1/8 inch OD was fit into the tank between the basket and tank wall. The cooling coil was connected to an external water bath kept at lower temperature (15°C ± 2°C). The implementation of this device provided better temperature control. However, the temperature still needed to be monitored, since the external water bath was not automatic or self-regulated. The external water bath temperature required to be adjusted every hour to an hour and a half to keep the ultrasonic bath temperature in the range of 23°C ± 2°C. In Figure 4-16 (a) the cooling coil can be observed.

Another alternative was studied to maintain the ultrasonic bath temperature constant. A pump was used to infuse fresh water from an external water bath into the tank through PVC hoses 5/16 inch ID, 7/16 inch OD. The second pump transported water from the tank to the external water bath. The water recirculation was helpful, but could only regulate temperature for short periods of time of 20 to 30 minutes. Figure 4-16 (b) shows the pump placed inside the ultrasonic bath and the hoses.

Two sections of PTFE column of 3/8 inch ID and 3 inches length were established for this study. Every section was packed with Low-Carbon Steel Balls, of 3/32 inch Diameter from McMaster-Carr. New spheres were used for every experiment. Table 4-6 presents the spheres material composition.

Table 4-6. Material composition of the carbon steel spheres

Material Composition	
Carbon	0.13-0.20%
Manganese	0.30-0.90%
Silicon	0.15-0.30%
Phosphorus	0.04% Max.
Sulfur	0.50% Max.
Iron	98.06-99.42%

Every column section was connected using straight connectors Durable Nylon Tube Fitting, Straight Connector for 1/2" Tube OD nut, a sleeve (ferrule), and a Buna-N O-ring from Mc-Master Carr. The O-rings function to provide sealing between sections. The Buna-N material has some chemical resistance limitations when exposed to toluene and/or heptane, for this reason new Buna-N O-rings were

used for each experiment. The use of FEP with Viton® Extreme-Chemical O-ring, from Mc-Master Carr was also validated. This type of O-ring is an alternative and can be used multiple times. Chemical-Resistant PFA straight connectors, including a nut, an ETFE gripping ring, and a PTFE sleeve (ferrule), were also evaluated, in an attempt to build a system in which all components had strong chemical resistant to the substances they were exposed to. However, the sealing offered by the PFA connectors was not very effective and the system presented leaks while in operation especially at precipitant to model oil ratio i.e. 90-10 as can be observed in Figure 4-17.

Figure 4-17. System leaks while in operation using Chemical resistant PFA straight connectors. 90-10 n-heptane to model oil A ratio, 12 ml/hr

To separate the spheres packed in each section a molded PTFE Mesh 0.045" x 0.025" Opening Size was used as a support. The mesh was located in the nut from the straight connector at the bottom part of each section. At the end of each experiment the column was drained by gravity and disassembled beginning from the top section to the bottom. In some cases, which will be discussed in section 4.4.2,

when the column could not be drained by gravity, compressed air was injected from the top section to induce the liquid inside the column to flow downstream.

After the device was disassembled, the column components were washed with toluene and /or dichloromethane – DCM and the liquid were collected on separate containers. Subsequently, the solvent was evaporated at 110°C placing the corresponding beaker or glass dishes on a heating plate. The previous process allowed quantifying the mass of asphaltene accumulated in the system components. The spheres were recovered separately per section on glass dishes and the solvent was evaporated at 110°C on a heating plate until constant weight was achieved. The weight gain by the spheres corresponded to the asphaltenes that precipitated and deposited on the metallic surface. Figure 4-18 (a) shows the PTFE column, Figure 4-18 (b) shows the detailed Nylon straight connector parts and Figure 4-18 (c) shows the PTFE mesh location.

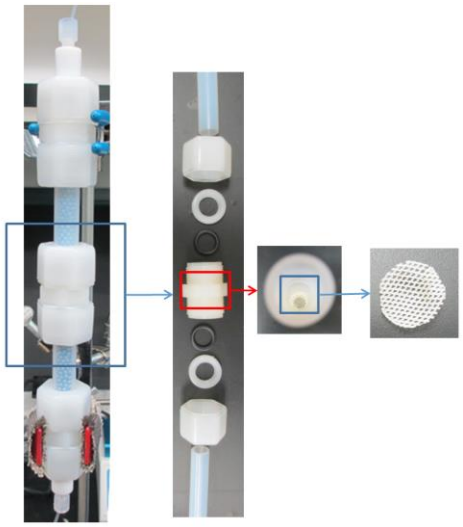

Figure 4-18. Column Detail. (a) PTFE Column (b) Detailed Nylon straight connector (c) PTFE mesh location

This novel apparatus offers an alternative option to traditional methodologies for evaluating actual asphaltene deposition on metallic surfaces. Evaluation with the new system is performed under more realistic conditions. Unlike current commercially available methods used to evaluate the effectiveness of asphaltene inhibitors, the proposed method allows for quantifying of actual deposition under dynamic conditions. Figure 4-19 shows a schematic on asphaltene deposition occurring inside the column sections. Figure 4-20 presents a schematic of the novel system to probe asphaltene deposition and Figure 4-21 shows the actual system.

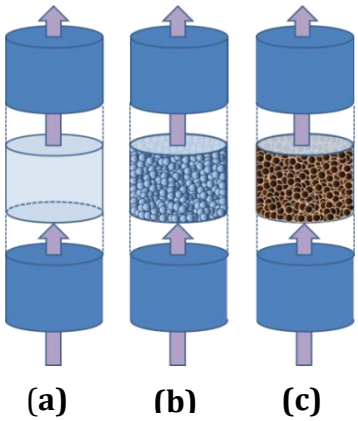

Figure 4-19. Novel system to probe asphaltene deposition at ambient conditions and under dynamic conditions. (a) The system is composed by multiple sections. Here the empty middle section is highlighted. (b) Each section was filled with carbon steel spheres, to increase the surface area and the amount of asphaltene that can potentially deposit. (c) A blend of crude oil and n-heptane flown through and the asphaltene deposited was collected and quantified.

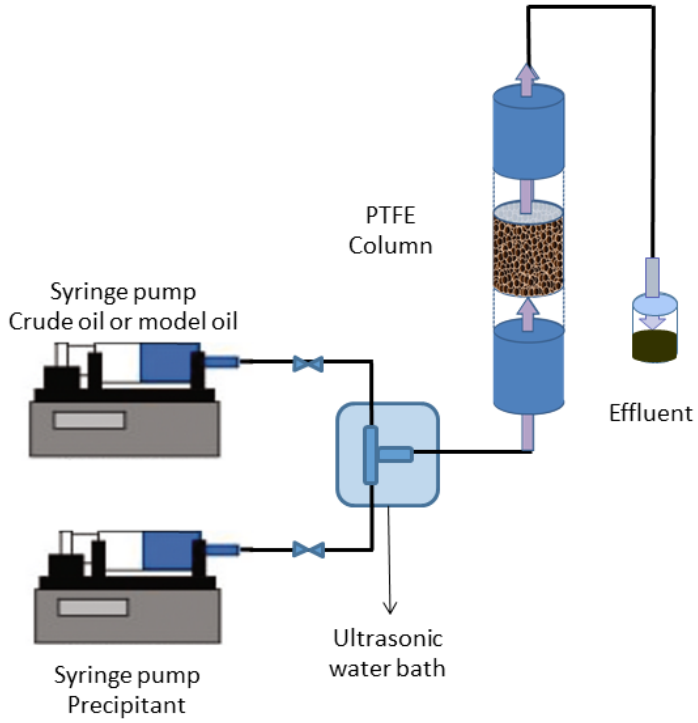

Figure 4-20. Schematic of the novel system to probe asphaltene deposition at ambient conditions and under dynamic conditions.

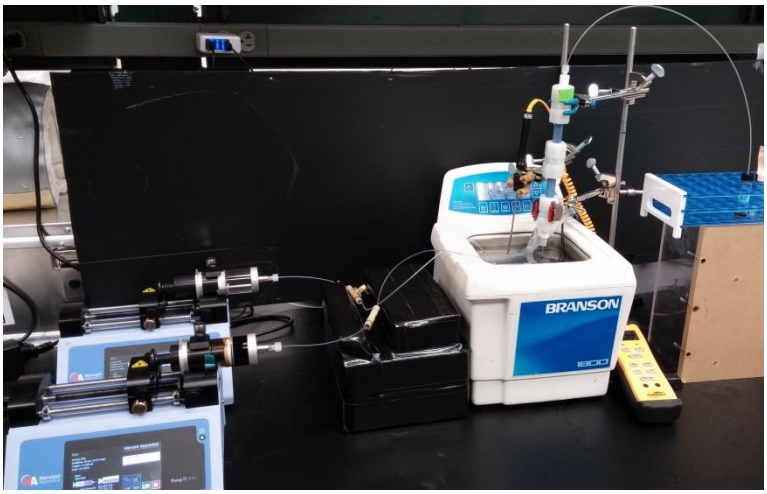

Figure 4-21. Novel system to probe asphaltene deposition at ambient conditions and under dynamics conditions.

4.4.2. Experimental procedure and results

In order to establish the best condition to operate the system model, oil A with 1 wt. % C_{5+} asphaltene content was used. The model oil preparation was done following the procedure described in section 4.1. Experiments at different precipitant to model oil ratio (70-30 and 90-10), time (6 hours and 12 hours) and flow rate (6 ml/h and 12 ml/h) were conducted at ambient pressure and temperature to establish reproducible operating conditions that enabled the quantification of the asphaltene deposit formed.

From Table 4-7 it can observed that for experiments at 90-10 precipitant to model oil ratio, 12 ml/h and 6 hours, the mass of asphaltene deposit obtained on the bottom section spheres was 16.1 ± 10.3 mg and 10.3 ± 8.2 mg on the spheres placed on the top section. When experiments were performed for 12 hours the mass of asphaltene deposit obtained in the bottom section spheres was 23.7 ± 1.2 mg. However, data for the amount of asphaltene deposited on the spheres of the top section 13.8 mg was reliable only for one experiment. Therefore, it was observed that tests performed at 90-10 precipitant to model oil A ratio did not have good repeatability at 6 hours nor 12 hours of total experiment time.

Subsequently, the precipitant to model oil ratio was reduced to 70-30 and the data obtained showed better repeatability. For 12 hours and 6 ml/h flow rate experiments the mass of asphaltene deposit on the carbon steel spheres was 20.8 ± 6.2 mg and 10.3 ± 4.2 mg for the bottom and top section respectively. Hence, keeping the precipitant to model oil ratio constant the flow rate was increased to 12

ml/h, reducing the experimental time to 6 hours. The amount of asphaltene deposit on the carbon steel spheres was 20.6 ± 1.4 mg and 8.0 ± 1.6 mg for the bottom and top section spheres.

According to these results, the more repeatable conditions were 70-30 model oil A to precipitant ratio, with a flow rate of 12 ml/h and total time of 6 hours. This suggests that at higher flow rates and shorter experimental times the results are more reliable and experiment conditions can be better controlled. Thus, these conditions were selected to test the effect of commercial asphaltene dispersants studied in sections 4.2 and 4.3 on the deposition of asphaltenes.

The pore volume is also reported in Table 4-7 and corresponds to the ratio between the total volume that flew through the system over the available volume ($V_{total} / V_{available}$) and represents the number of times the column was filled. From Table 4-7 it is observed that when the pore volume was duplicated the amount of asphaltene deposit obtained was not very reproducible.

Table 4-7. Evaluation of the operation conditions with model oil A with an asphaltene content of 1 wt. % *Result for a single experiment

Operation conditions				Asphaltene Deposit on Spheres Surface (mg)	
Model Oil A - Precipitant ratio	Flow Rate (ml/h)	t (h)	Pore Volume	Bottom Section	Top Section
70-30	12	6	15	20.6 ± 1.4	8.0 ± 1.6
	6	12	15	20.8 ± 6.2	10.3 ± 4.2
90-10	12	6	15	16.1 ± 10.3	10.3 ± 8.2
	12	12	30	23.7 ± 1.2	13.8*

Table 4-8 shows the amount of asphaltenes accumulated in each component of the column for the model oil A evaluated at the established operation conditions of 70-30 model oil to precipitant ratio, 12 ml/h for a total time of 6 hours. The system components with the most asphaltene accumulation were the two PTFE sections of column and the PTFE mesh that is placed at the bottom section to support the spheres.

Table 4-8. Asphaltene accumulation on the system components for the model oil A evaluated at 70-30 model oil to precipitant ratio, 12 ml/h and 6h

System Component	Asphaltene Deposit (%)
Column Bottom Section	3.7 ± 0.5
Column Top Section	2.6 ± 0.8
Mesh Bottom Section	1.4 ± 1.0
Mesh Top Section	0.1 ± 0.1
Adapters (Bottom and Top)	0.1 ± 0.1

In order to study the effect of the asphaltene commercial dispersants 8, 9 and 15 on asphaltene deposition, blends of crude oil S with and without dispersants 8, 9 and 15 were prepared following the same procedure that was explained in section 4.2.1. The experiments were performed at operation established conditions of precipitant to treated or untreated crude oil S ratio of 70:30 vol. % with a constant flow rate of 12 ml/h for 6 hours, at ambient conditions of temperature and pressure. Due to sample availability limitations, each test was performed once. Table 4-9 presents the results for dispersants 8, 9 and 15 at 100 ppm. The dosage of 100 ppm was chosen to compare the results with HPHT experiments for dispersant 9 discussed in section 3.1.2.

Table 4-9. Dispersant effect on asphaltene deposition for Crude Oil S evaluated at 70-30 crude oil to precipitant ratio, 12 ml/h and 6h

	Asphaltene deposit (mg)			
	Blank	Disp. 8 100 ppm	Disp. 9 100 ppm	Disp. 15 100 ppm
Bottom Section Spheres	60.9	95.5	59.0	26.0
Top Section Spheres	31.0	25.5	28.6	23.0
Total	91.9	121	87.6	49

When asphaltene deposition is evaluated using the new system, it can be observed from Table 4-9 that when crude oil S is treated with dispersant 15 at 100 ppm the amount of asphaltene deposit that is generated (49 mg) is smaller than the amount generated by the blank (91.9 mg). From the results obtained in section 4.2, dispersant 15 was ranked as the weakest dispersant. Thus, traditionally it would be dismissed as a good candidate to prevent asphaltene deposition. However, the results obtained using the new asphaltene deposition evaluation system proposed in this work suggest the opposite. In this case, a weak asphaltene dispersant performs as a good asphaltene deposition inhibitor.

Dispersant 8 was ranked in section 4.2 as the best dispersant. However, according to the results presented in Table 4-9 when the crude oil was treated with dispersant 8 at 100 ppm and tested on the PTFE column system, the amount of asphaltene deposit accumulated on the spheres surface was the maximum obtained in all cases (121 mg). Thus, this presents evidence that a good dispersant does not necessarily perform as a good asphaltene deposition inhibitor. On the contrary, as in the case of dispersant 8, a good dispersant can make the asphaltene deposition

worse. After the test was completed, the column was disassembled and the visual inspection of the column components provided additional evidence of the asphaltene deposit formation. Figure 4-22 (a) shows the bottom PTFE adapter that corresponds to the reducer connector that attaches the column inlet to the PFA tubing that carries the precipitant oil blend. Figure 4-23 (a) shows the PTFE bottom section mesh visual observation. The presence of a black solid layer accumulated on the top surface of the pieces evidences the asphaltene deposit formation.

(a) (b)

Figure 4-22. Bottom adapter – Reducer connector. Visual inspection after test completion. Crude oil S evaluated at 70-30 precipitant to oil ratio, 12 ml/h and 6h treated with (a) 100 ppm of dispersant 8 (b) 500 ppm of dispersant 9

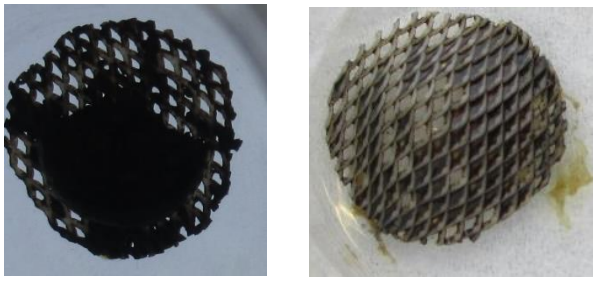

(a) **(b)**

Figure 4-23. Bottom section PTFE Mesh visual observation after test completion. Crude oil S evaluated at 70-30 precipitant to oil ratio, 12 ml/h and 6h treated with (a) 100 ppm of dispersant 8 (b) 500 ppm of dispersant 9

SDS results presented in section 3.1.2 considered dispersant 9 at 100 ppm a good asphaltene deposition inhibitor for crude oil A, which comes from the same field as crude oil S. For the same dispersant dosage Table 4-9 shows that when crude oil S is treated with dispersant 9 the amount of asphaltene deposit (87.6 mg) is slightly lower than that generated by the blank (91.9 mg). In other words, dispersant 9 dos not seem to significantly reduce the asphaltene deposition for the crude oil S under these conditions.

Table 4-10. Dispersant dosage effect on asphaltene deposition for Crude Oil S evaluated at 70-30 crude oil to precipitant ratio, 12 ml/h and 6h

	Asphaltene deposit (mg)		
	Blank	Disp. 9 100 ppm	Disp. 9 500 ppm
Bottom Section Spheres	60.9	59.0	68.5
Top Section Spheres	31.0	28.6	32.6*
Total	91.9	87.6	101.1

In section 4.2 it was found that increasing the dispersant 9 dosage improved its efficiency. As has been previously discussed, the effect of a good dispersant on the asphaltene aggregation consists on slowing down the aggregation rate. According to the mechanism for asphaltene deposition presented in section 2.3, asphaltene aggregation and deposition of asphaltenes seem to be competing phenomena, meaning the higher the aggregation the lower the deposition. Table 4-9 shows that treating the crude oil S with 500 ppm of dispersant 9 produced an amount of formed deposit (101.1 mg) greater than the one generated by the untreated crude oil S (91.6 mg). However, when the crude oil was treated with a

lower dosage of 100 ppm of dispersant 9 the amount of deposit was slightly lower (87.6 mg) than the one obtained from untreated crude oil (91.6 mg). Therefore, in the case of dispersant 9, the dosage effect on asphaltene deposition does not seem to be conclusive. Figure 4-22 (b) shows the visual observation for the bottom PTFE adapter at the conclusion of the experiment when the column was disassembled. Figure 4-23 (b) shows the PTFE bottom section mesh visual observation. The presence of the black solid layer accumulated on the top surface of the pieces evidences asphaltene deposit formation.

Table 4-11. Asphaltene accumulation (%) on the system components for treated and untreated crude oil S evaluated at 70-30 crude oill to precipitant ratio, 12 ml/h and 6h

	Asphaltene deposit by Components (mg)				
System Components	Blank	Disp. 8 100 ppm	Disp. 9 100 ppm	Disp. 15 100 ppm	Disp. 9 500 ppm
Bottom Section Spheres	60.9	95.5	59.0	26.0	68.5
Top Section Spheres	31.0	25.5	28.6	23.0	32.6
Column Bottom Section	20.6	70.6	8.7	25.2	41.1
Column Top Section	21.1	55.3	26.6	20.8	43.4
Mesh Bottom Section	7.9	27	1.9	7.3	2.5
Mesh Top Section	0.7	3.3	2.3	4.2	1.5
Adapters (Bottom + Top)	3.9	23.4	0.6	2.8	1.7
Total (mg)	146.1	300.6	127.7	109.3	191.3

Table 4-11 shows the amount of asphaltenes accumulated in each component of the column for the crude oil S and crude oil S treated with dispersants 8, 9 and 15. After every experiment was completed, it was observed that, in addition to the carbon steel spheres, the components that accumulate the majority of asphaltenes

deposit formation are the PTFE column sections followed by the bottom mesh and the adapters.

The amount of deposit formation quantified on the spheres and the column components ranged between 109.3 mg for the system treated with 100 ppm of dispersant 15, to 146.1 mg for the untreated system from the total 200 mg of C_{7+} asphaltenes injected initially to the system. The remaining asphaltenes exit the system and are collected on the effluent. The previous results show that not all the asphaltenes that precipitate further deposit. There is a fraction of asphaltenes available that precipitate but do not form asphaltene deposits and are transported throughout the column by the flow to the effluent.

From Table 4-11 it is observed that the total amount of asphaltenes accumulated in system components and the spheres surface for the system treated with 100 ppm of dispersant 8 300.6 mg, constitute more than the initial 200 mg from the C_{7+} asphaltenes which were destabilized by the n-heptane addition. Unlike model oil systems where the only components are the solvent and the asphaltenes, crude oil systems are much more complex. The crude oil sample becomes more unstable at ambient conditions with time. The test with dispersant 8 at 100 ppm was the last test performed. The crude oil aging-time effect that destabilizes the sample could be reflected on the total mass of deposit formation. Another consideration to take into account is that the draining process of the column was different when the crude oil was treated with dispersants 8 and 9. Compressed air

injection was required to drain the column, since the process could not be driven only by gravity.

For all the systems evaluated, Table 4-11 shows that asphaltene deposit formation on the carbon steel spheres - which provide the metallic surface for asphaltene deposition -, occur primarily in spheres located in the bottom section of the column. Therefore, the deposit formation is not homogenous as had been assumed in previous works.

In section 4.2.1 dispersants 8, 9 and 15 were ranked according to their dispersive efficiency. Dispersant 8 was ranked as the best, followed by dispersant 9 and dispersant 15. Based on results obtained with the PTFE column for evaluating asphaltene deposition formation, the trend is the opposite; dispersant 15 appears to be the best asphaltene deposition inhibitor followed by dispersant 9 and dispersant 8. As previously mentioned, previous asphaltene deposition experiments were performed once due to sample limitations. Hence, it is important to highlight that these results need further validation.

While the system developed in this work constitutes an initial prototype and still has some limitations, it was especially useful for determining the performance of commercial asphaltene dispersants studied in section 4.2 and 4.3. It also made possible quantifying the amount of asphaltene deposited on the spheres surface. The comparison of these results to observations discussed in previous sections offers valuable and promising information on the study of asphaltene – inhibitor interactions.

Chapter 5

Conclusions and Recommendations

5.1. Conclusions

Asphaltene precipitation, aggregation and deposition are part of a complex multi-step mechanism that it is still under active investigation. In this work, precipitation of asphaltene is defined as the separation of a distinct asphaltene rich-phase from an asphaltene lean-phase. Asphaltene particles, as small as a few hundred nanometers, begin to form at the onset of asphaltene precipitation. These small particles can either further aggregate or get dispersed and eventually deposit on an available surface. According to the results presented in this work, commercial asphaltene dispersants interact with the asphaltenes in the oil to slow down the asphaltene aggregation rate. Conventional techniques, based on NIR transmittance or optical microscopy, are unable to detect the onset of asphaltene precipitation, due to their insufficient sensitivity and, consequently, they may provide misleading

results that suggest the addition of the inhibitor causes a shift in the thermodynamic stability of asphaltenes. Actually, the precipitation of asphaltenes occurs at the same ratio of oil/n-heptane for treated and untreated systems, according to the results obtained with the indirect method, which is approximately one order of magnitude more sensitive than conventional techniques used to determine the onset of asphaltene precipitation. The experimental evidence shows that asphaltene dispersants neither shift the actual onset of asphaltene precipitation nor reduce the amount of asphaltene precipitated. Because the precipitation of asphaltenes is not affected by the dispersant, dispersion efficiency should not be evaluated considering the shift in the detection of asphaltene precipitation as the evaluation parameter.

Also, analysis of the performance of chemicals used to disperse asphaltenes is usually done through the asphaltene dispersion test (ADT), which analyzes dead oil samples at ambient conditions. Also, ADT requires a high dilution with n-heptane. The results presented in this work provide experimental evidence against the reliability of ADT. For example, experiments performed at 25 and 70°C reveal that the maximum efficiency of dispersants is reduced for increasing temperatures. This can be due to the effect of temperature on the ability of the chemical to disperse asphaltenes, or simply because, in general, the solubility of asphaltenes increases with temperature and therefore the addition of a dispersant provides a reduced benefit for more stables systems. In either case the ranking of chemicals based on their performance can be greatly affected by the temperature at which the experiments are conducted. The same is true for the effect of the concentration of

blends analyzed. In ADT, oil, with or without dispersant, is mixed with n-heptane to produce blends than contain up to 97% of n-heptane. The performance of the chemical was also found to be highly dependent on the ratio of n-heptane to oil. Thus, a successful method to analyze and rank the performance of asphaltene dispersants at ambient pressure should take, as a minimum, the effect of temperature and composition into consideration.

The dispersive performance was introduced as a new index to evaluate the dispersants formulations efficiency. It allows ranking and comparing different dispersant formulations under the same conditions. The results collected through this index agree with observations from the graphical analysis. As expected, the dispersive performance of all the chemicals increased with increasing concentration of dispersant. At 500 ppm the three commercial inhibitors that were tested behaved similarly, and only one held this performance at concentrations as low as 70 ppm. Thus, it is recommended to investigate the performance of chemicals at the lower concentrations, such as 50 to 100 ppm, which is a more desirable formulation from an economic perspective.

A new system to evaluate asphaltene deposition was developed in this work. The system constitutes a promising alternative to study asphaltene deposition under more realistic conditions. The system allows evaluation of asphaltene deposition under dynamic conditions at ambient conditions. The small amount of samples required for testing represents an advantage. Also, based on the design developed in this work there is promising adaptability to work at high pressure and

high temperature in order to mimic reservoir conditions. The current system offers the flexibility to study different asphaltene deposition inhibitor formulations, as well as asphaltene deposition on different type of materials to test various surface types, and roughness to investigate actual pipeline materials and coatings. These results notwithstanding, there is space for improvement on the repeatability and accuracy of the results. These types of studies would help validate the fact that experiments at ambient conditions could be extended to more realistic conditions of composition, temperature and pressure.

There is not a direct correlation between “good dispersant” and its capability to prevent asphaltene deposition. A weak dispersant can perform as a good asphaltene deposition inhibitor and vice versa.

The results presented in this dissertation offer promising new alternatives for screening and selecting asphaltene deposition inhibitors. Several lessons have been learned and the experimental data provide insight into the effect of asphaltene dispersants on the asphaltene precipitation, aggregation and deposition phenomena. This knowledge would contribute to the development of experimental procedures and simulation schemes that could predict the likelihood of asphaltene deposition.

5.2. Recommendations

The new system developed to evaluate asphaltene deposition can be used in the near future to provide additional insight into the effects of different flow rates, precipitant to oil ratio, aging time, water and temperature on asphaltene deposition. In order to study these effects, there are still system limitations that need to be address.

To ensure well defined thermal conditions in the ultrasonic water bath and improve temperature control, an ultrasonic water bath with automate cooling system should be implemented. This would also eliminate the need of permanent supervision.

The amount of asphaltene deposit accumulated in the PTFE mesh can be minimized, reducing the mesh surface area. In order to do so, an alternative mesh with a larger opening size (0.045 inch < Mesh opening size < 3/32 inch) should be implemented.

The carbon steel spheres recovery and drying process is susceptible to further improvement as well. An alternative methodology to minimize risk of losing spheres when they are recovered should be incorporated. In addition, the draining process of the column at the end of the experiment requires additional work. Alternative ways of draining the column such as the use of nitrogen instead of compressed air, or only gravity should be explored.

Due to the fact that the ultimate objective is to predict the effectiveness of asphaltene deposition inhibitors on preventing actual asphaltene deposition, the effect of asphaltene deposition inhibitors needs to be tested at reservoir conditions of high temperature and high pressure. A system consisting of a stainless steel column of 1 inch ID and 1 ft. height, currently used to study asphaltene deposition in porous media, can be adapted and used to study asphaltene deposition on metallic surfaces by replacing the sand for carbon steel spheres. In the current design the precipitant and oil blend are injected through the column using a couple of ISCO pumps that allow reaching pressure up to 5000 psi. To achieve high temperatures the column can be located inside a Blue M Electric oven to reach temperatures up to 250°F equivalent to 12°C. The system operates very similarly to the design presented in this work. Precipitation is induced by the addition of n-heptane and the oil and precipitant are mixed in a T-Junction immersed in an ultrasonic water bath to promote good mixing.

Figure 5-1. HPHT Stainless steel column for the study of asphaltene deposition.

The implementation of the recommendations will contribute to the improvement of the accuracy and precision of the system to generate reproducible and reliable results.

References

1. Wiehe, I. A. Asphaltene solubility and fluid compatibility. *Energy & Fuels* **26,** 4004–4016 (2012).

2. Vargas, F. M. Modeling of Asphaltene Precipitation and Arterial Deposition. (Rice University, 2009).

3. Jewell, D. M., Weber, J. H., Bunger, J. W., Plancher, H. & Latham, D. R. Ion-Exchange, Coordination, and Adsorption Chromatographic Separation of Heavy-End Petroleum Distillates. *Anal Chem* **44,** 1391–1395 (1972).

4. Wang, J. X. Predicting Asphaltene Flocculation in Crude Oils. (New Mexico Institute of Mining & Technology, 2000).

5. Kabir, C. S., Jamaluddin, A. K. M. & others. Asphaltene characterization and mitigation in south Kuwait's Marrat reservoir. *SPE production & facilities* **17,** 251–258 (2002).

6. León, O., Rogel, E., Espidel, J. & Torres, G. Asphaltenes: Structural Characterization, Self-Association, and Stability Behavior. *Energy Fuels* **14,** 6–10 (2000).

7. Calemma, V., Iwanski, P., Nali, M., Scotti, R. & Montanari, L. Structural Characterization of Asphaltenes of Different Origins. *Energy Fuels* **9,** 225–230 (1995).

8. Ancheyta, J. *et al.* Extraction and Characterization of Asphaltenes from Different Crude Oils and Solvents. *Energy Fuels* **16,** 1121–1127 (2002).

9. Wu, J., Prausnitz, J. M. & Firoozabadi, A. Molecular-thermodynamic framework for asphaltene-oil equilibria. *AIChE J.* **44,** 1188–1199 (1998).

10. Vargas, F. M., Creek, J. L. & Chapman, W. G. On the Development of an Asphaltene Deposition Simulator. *Energy Fuels* **24,** 2294–2299 (2010).

11. Rocha Junior, L. C., Ferreira, M. S. & da Silva Ramos, A. C. Inhibition of asphaltene precipitation in Brazilian crude oils using new oil soluble amphiphiles. *Journal of Petroleum Science and Engineering* **51,** 26–36 (2006).

12. Zougari, M. I., Ratulowski, J., Hammami, A. & Kharrat, A. Live Oils Novel Organic Solid Deposition and Control Device: Wax and Asphaltene Deposition Validation. in (Society of Petroleum Engineers, 2005). doi:10.2118/93558-MS

13. Juyal, P., Ho, V., Yen, A. & Allenson, S. J. Reversibility of Asphaltene Flocculation with Chemicals. *Energy Fuels* **26,** 2631–2640 (2012).

14. Abrahamsen, E. L. Organic flow assurance: Asphaltene dispersant/inhibitor formulation development through experimental design. (2012). at <http://brage.bibsys.no/xmlui/handle/11250/182547>

15. Lighfford, S., Pitoni, E., Armesi, F. & Mauri, L. Development and field use of a novel solvent/water emulsion for the removal of asphaltene deposits in fractured carbonate formations. *SPE Prod. Oper.* **23,** 301–311 (2008).

16. Rogel, E. Effect of Inhibitors on Asphaltene Aggregation: A Theoretical Framework†. *Energy & Fuels* **25,** 472–481 (2010).

17. Ibrahim, H. H. & Idem, R. O. Interrelationships between Asphaltene Precipitation Inhibitor Effectiveness, Asphaltenes Characteristics, and Precipitation Behavior during n-Heptane (Light Paraffin Hydrocarbon)-Induced Asphaltene Precipitation. *Energy Fuels* **18,** 1038–1048 (2004).

18. Trbovich, M. G., King, G. E. & others. Asphaltene Deposit Removal: long-lasting treatment with a Co-solvent. in *SPE International Symposium on Oilfield Chemistry* (Society of Petroleum Engineers, 1991). at <https://www.onepetro.org/conference-paper/SPE-21038-MS>

19. Ghloum, E. F., Al-Qahtani, M. & Al-Rashid, A. Effect of inhibitors on asphaltene precipitation for Marrat Kuwaiti reservoirs. *Journal of Petroleum Science and Engineering* **70,** 99–106 (2010).

20. Eskin, D., Ratulowski, J., Akbarzadeh, K. & Pan, S. Modelling asphaltene deposition in turbulent pipeline flows. *Can. J. Chem. Eng.* **89,** 421–441 (2011).

21. González, Fabio A. Personal communication. Asphaltene deposition economic impact. Reservoir Performance Global Community of Practice Lead BP. (2015).

22. Abdallah, Dalia S. Personal communication. Abu Dhabi Company for Onshore Petroleum Operations Ltd., Abu Dhabi, UAE. (2015).

23. Akbarzadeh, K. *et al.* The importance of asphaltene deposition measurements in the design and operation of subsea pipelines. in *SPE annual technical conference and exhibition* 4–7 (2009). at <https://www-onepetro-org.ezproxy.rice.edu/download/conference-paper/SPE-124956-MS?id=conference-paper%2FSPE-124956-MS>

24. Wang, J., Buckley, J. S. & Creek, J. L. Asphaltene deposition on metallic surfaces. *J. Dispers. Sci. Technol.* **25,** 287–298 (2004).

25. Hashmi, S. M., Loewenberg, M. & Firoozabadi, A. Colloidal asphaltene deposition in laminar pipe flow: Flow rate and parametric effects. *Physics of Fluids (1994-present)* **27,** 083302 (2015).

26. Vargas, F. M. *et al.* Advances in Understanding Asphaltene Precipitation and Deposition. in (2014).

27. Mullins, O. C. The Modified Yen Model†. *Energy Fuels* **24,** 2179–2207 (2010).

28. Mullins, O. C. *et al.* Advances in asphaltene science and the Yen–Mullins model. *Energy Fuels* **26,** 3986–4003 (2012).

29. Tavakkoli, M. *et al.* Indirect Method: A Novel Technique for Experimental Determination of Asphaltene Precipitation. *Energy Fuels* **29,** 2890–2900 (2015).

30. Haskett, C. E. & Tartera, M. A Practical Solution to the Problem of Asphaltene Deposits-Hassi Messaoud Field, Algeria. *J. Pet. Sci. Eng.* **17,** 387–391 (1965).

31. Allenson, S. J. & Walsh, M. A. A Novel Way to Treat Asphaltene Deposition Problems Found in Oil Production. in (Society of Petroleum Engineers, 1997). doi:10.2118/37286-MS

32. Thomas, D. C., Becker, H. L. & Del Real Soria, R. A. Controlling Asphaltene Deposition in Oil Wells. *SPE Production & Facilities* **10,** 119–123 (1995).

33. Garcia, M. C., Chiaravallo, N., Sulbaran, A., El Chiriti, K. & Chirinos, A. Production Restarting on Asphaltene-Plugged Oil Wells in a Lake Maracaibo Reservoir. in (Society of Petroleum Engineers, 2001). doi:10.2118/69513-MS

34. Allen, T. O. & Roberts, A. P. *Production Operation (Well Completions, Workover, and Stimulation)*. (Oil & Gas Consultants International, Inc., 1982).

35. Hirschberg, A., DeJong, L. N. J., Schipper, B. A. & Meijer, J. G. Influence of Temperature and Pressure on Asphaltene Flocculation. *SPE J* **24,** 283–293 (1984).

36. Newberry, M. E. & Barker, K. M. Formation Damage Prevention Through the Control of Paraffin and Asphaltene Deposition. in (Soc. Pet. Eng., 1985). doi:10.2118/13796-MS

37. González, G. & Middea, A. Peptization of asphaltene by various oil soluble amphiphiles. *Colloids and Surfaces* **52,** 207–217 (1991).

38. Wang, J., Li, C., Zhang, L., Que, G. & Li, Z. The Properties of Asphaltenes and Their Interaction with Amphiphiles. *Energy Fuels* **23,** 3625–3631 (2009).

39. Yen, A., Yin, Y. R. & Asomaning, S. Evaluating Asphaltene Inhibitors: Laboratory Tests and Field Studies. in (Society of Petroleum Engineers, 2001). doi:10.2118/65376-MS

40. Barcenas, M., Orea, P., Buenrostro-González, E., Zamudio-Rivera, L. S. & Duda, Y. Study of Medium Effect on Asphaltene Agglomeration Inhibitor Efficiency. *Energy Fuels* **22,** 1917–1922 (2008).

41. Smith, D. F. *et al.* Crude Oil Polar Chemical Composition Derived from FT–ICR Mass Spectrometry Accounts for Asphaltene Inhibitor Specificity. *Energy Fuels* **22,** 3112–3117 (2008).

42. Barcenas, M. & Orea, P. Molar-Mass Distributions of Asphaltenes in the Presence of Inhibitors: Experimental and Computer Calculations. *Energy Fuels* **25,** 2100–2108 (2011).

43. Chang, C.-L. & Fogler, H. S. Stabilization of Asphaltenes in Aliphatic Solvents Using Alkylbenzene-Derived Amphiphiles. 1. Effect of the Chemical Structure of Amphiphiles on Asphaltene Stabilization. *Langmuir* **10,** 1749–1757 (1994).

44. Chang, C.-L. & Fogler, H. S. Stabilization of Asphaltenes in Aliphatic Solvents Using Alkylbenzene-Derived Amphiphiles. 2. Study of the Asphaltene-Amphiphile Interactions and Structures Using Fourier Transform Infrared Spectroscopy and Small-Angle X-ray Scattering Techniques. *Langmuir* **10,** 1758–1766 (1994).

45. Kraiwattanawong, K. *et al.* Effect of Asphaltene Dispersants on Aggregate Size Distribution and Growth. *Energy Fuels* **23,** 1575–1582 (2009).

46. Oschmann, H.-J. *et al. Chemistry in the Oil Industry VII: Performance in a chellenging enviroment. New Methods for the Selection of Asphaltene Inhibitors in the Field. SPECIAL PUBLICATION-ROYAL SOCIETY OF CHEMISTRY*. (2002).

47. Kelland, M. A. *Production Chemicals for the Oil and Gas Industry*. (CRC Press, 2009).

48. Chávez-Miyauchi, T. E., Zamudio-Rivera, L. S., Barba-López, V., Buenrostro-Gonzalez, E. & Martínez-Magadán, J. M. N-aryl amino-alcohols as stabilizers of asphaltenes. *Fuel* **110,** 302–309 (2013).

49. Al-Sahhaf, T. A., Fahim, M. A. & Elkilani, A. S. Retardation of asphaltene precipitation by addition of toluene, resins, deasphalted oil and surfactants. *Fluid Phase Equilibria* **194–197,** 1045–1057 (2002).

50. Oh, K. & Deo, M. D. Effect of Organic Additives on the Onset of Asphaltene Precipitation. *Energy Fuels* **16,** 694–699 (2002).

51. Goual, L., Sedghi, M., Wang, X. & Zhu, Z. Asphaltene Aggregation and Impact of Alkylphenols. *Langmuir* **30,** 5394–5403 (2014).

52. Mohammadi, M. *et al.* Inhibition of Asphaltene Precipitation by TiO2, SiO2, and ZrO2 Nanofluids. *Energy Fuels* **25,** 3150–3156 (2011).

53. Carnahan, N. F., Salager, J.-L., Antón, R. & Dávila, A. Properties of Resins Extracted from Boscan Crude Oil and Their Effect on the Stability of Asphaltenes in Boscan and Hamaca Crude Oils. *Energy Fuels* **13,** 309–314 (1999).

54. Fuhr, B. J., Klein, L. L. & Reichert, C. Measurement Of Asphaltene Flocculation In Bitumen Solutions. *J Can Pet Technol* **25,** (1986).

55. Tavakkoli, M., Chen, A. & Vargas, F. M. Rethinking the modeling approach for asphaltene precipitation using the PC-SAFT Equation of State. *Fluid Phase Equilibria* **http://doi.org/FPE-S-15-00892,**

56. Akbarzadeh, K., Eskin, D., Ratulowski, J. & Taylor, S. Asphaltene Deposition Measurement and Modeling for Flow Assurance of Tubings and Flow Lines. *Energy Fuels* **26,** 495–510 (2012).

57. Boek, E. S., Ladva, H. K., Crawshaw, J. P. & Padding, J. T. Deposition of Colloidal Asphaltene in Capillary Flow: Experiments and Mesoscopic Simulation†. *Energy Fuels* **22,** 805–813 (2008).

58. Rahmani, N. H. G., Masliyah, J. H. & Dabros, T. Characterization of asphaltenes aggregation and fragmentation in a shear field. *AIChE J.* **49,** 1645–1655 (2003).

59. Broseta, D. *et al.* Detection of Asphaltene Deposition by Capillary Flow Measurements. in *SPE/DOE Improved Oil Recovery Symposium* (Soc. Pet. Eng., 2000). at <https://www.onepetro.org/conference-paper/SPE-59294-MS>

60. Hoepfner, M. P., Limsakoune, V., Chuenmeechao, V., Maqbool, T. & Fogler, H. S. A fundamental study of asphaltene deposition. *Energy & Fuels* **27,** 725–735 (2013).

61. Nabzar, L. & Aguiléra, M. E. The Colloidal Approach. A Promising Route for Asphaltene Deposition Modelling. *Oil & Gas Science and Technology - Revue de l'IFP* **63,** 21–35 (2008).

62. Peramanu, S., Singh, C., Agrawala, M. & Yarranton, H. W. Investigation on the Reversibility of Asphaltene Precipitation. *Energy Fuels* **15,** 910–917 (2001).

63. Peramanu, S., Clarke, P. F. & Pruden, B. B. Flow loop apparatus to study the effect of solvent, temperature and additives on asphaltene precipitation. *Journal of Petroleum Science and Engineering* **23,** 133–143 (1999).

64. Soulgani, B. S., Rashtchian, D., Tohidi, B. & Jamialahmadi, M. Integrated Modelling Methods for Asphaltene Deposition in Wellstring. *J. Jpn. Pet. Inst.* **52,** 322–331 (2009).

65. Lawal, K. A., Crawshaw, J. P., Boek, E. S. & Vesovic, V. Experimental Investigation of Asphaltene Deposition in Capillary Flow. *Energy & Fuels* **26,** 2145–2153 (2012).

66. Lin, Y. J. *et al.* Probing Asphaltene Deposition Using Microfluidic Devices. in (2015).

67. Zougari, M. *et al.* Novel Organic Solids Deposition and Control Device for Live-Oils: Design and Applications. *Energy & Fuels* **20,** 1656–1663 (2006).

68. Akbarzadeh, K., Eskin, D., Ratulowski, J. & Taylor, S. D. Asphaltene Deposition Measurement and Modeling for Flow Assurance of Subsea Tubings and Pipelines. in (Offshore Technology Conference, 2011). doi:10.4043/22316-MS

69. Tavakkoli, M., Panuganti, S. R., Taghikhani, V., Pishvaie, M. R. & Chapman, W. G. Asphaltene Deposition in Different Depositing Environments: Part 2. Real Oil. *Energy Fuels* **28,** 3594–3603 (2014).

70. Maqbool, T., Balgoa, A. T. & Fogler, H. S. Revisiting asphaltene precipitation from crude oils: A case of neglected kinetic effects. *Energy Fuels* **23,** 3681–3686 (2009).

71. Vargas, F. M., Gonzalez, D. L., Hirasaki, G. J. & Chapman, W. G. Modeling Asphaltene Phase Behavior in Crude Oil Systems Using the Perturbed Chain

Form of the Statistical Associating Fluid Theory (PC-SAFT) Equation of State†. *Energy Fuels* **23,** 1140–1146 (2009).

72. Vargas, F. *et al.* On the Development of an Enhanced Method to Predict Asphaltene Precipitation. in (Offshore Technology Conference, 2014). doi:10.4043/25294-MS

73. Favero, C. V., Phichphimok, P. & Larson, R. G. A new approach to measure asphaltene deposition. in (2015).

74. Geankoplis, C. J. *Transport Process and Unit Operations*. (Prentice Hall, 2003).

Appendix A. Direct Method Correction of the Dilution Effect

In this section the procedure to correct the dilution effect is explained for the direct method. The details for the correction of the dilution effect for indirect method are reported by Tavakkoli et al. [29] Figure A-1 shows the raw data collected from the UV-Vis NIR spectrophotometer for the direct method before correction of the dilution effect, for a crude oil S with an asphaltene concentration of 2.8 w.t% C_{5+} asphaltenes and blends with different amounts of n-heptane, at room temperature and aged for 1 hour. It can be observed that all the spectra are noise-free in the whole wavelength range and no signal saturation can be observed. Therefore, all wavelengths in Figure A-1 can be used for post-processing of the raw data.

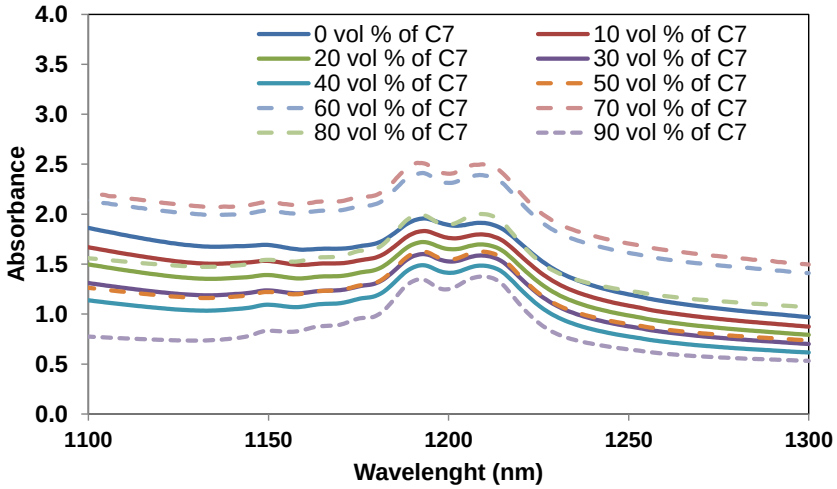

Figure A-1. Raw spectroscopy data for the direct method applied to a crude oil with asphaltene concentration of 2.8 wt. % diluted with n-heptane (C_7) and aged for 1 hour

To process the raw data shown in Figure A-1, a wavelength of 1100 nm was chosen. The wavelengths of 1100 nm to 1300 nm in the NIR region are good options for performing absorbance measurements, because pure heptane shows very small absorbance values in these two wavelengths and post-processing of the data is a straight forward procedure.

There is a step in the direct method dilution of the oil occurs: by addition of the precipitant, e.g. n-heptane. To properly correct the overall dilution effect the exact volumes of oil and added precipitant were required. For this purpose, the mass of each liquid was measured to back-calculate the corresponding volumes after each step in the sample preparation procedure. Ideal solution is assumed in these calculations. The values of 0.681 g/cm^3 and 0.843 g/cm^3 were used for the density of n-heptane and crude oil S at ambient temperature. Table A-1 presents the step by step calculation of the dilution of crude oil and n-heptane used to study asphaltene aggregation from the crude oil S with asphaltene concentration of 2.8 wt. % diluted with n-heptane and aged for 1 hour. The total volume of each sample is 3 ml. ideal mixing is assumed for the calculation of the dilution effect.

The dilution ratio caused by the addition of n-heptane to the crude oil sample represents the overall dilution ratio for this method.

Table A-2 shows the procedure to calculate the corrected absorbance values considering the overall dilution.

Table A-1. Calculation of the dilution effect caused by the addition of n-heptane (C_7) to the Crude Oil S

Expected vol. % of C_7	Crude oil mass (g)	C_7 mass (g)	Crude oil vol. (cm^3)	Heptane vol. (cm^3)	Heptane vol. % *	Dilution Ratio for C_7 addition **
0	4.2668	0.0000	5.0614	0.0000	0.0000	1.0000
10	3.7769	0.3585	4.4803	0.5264	10.5145	1.1175
20	3.3449	0.6789	3.9679	0.9969	20.0798	1.2512
30	2.9383	1.0322	3.4855	1.5157	30.3067	1.4349
40	2.4965	1.3686	2.9614	2.0097	40.4272	1.6786
50	2.1152	1.7236	2.5091	2.5310	50.2168	2.0087
60	1.6890	2.0602	2.0036	3.0253	60.1584	2.5099
70	1.2583	2.4171	1.4926	3.5493	70.3957	3.3779
80	0.8619	2.7602	1.0224	4.0532	79.8561	4.9643
90	0.4261	3.1216	0.5055	4.5838	90.0683	10.0687

$$*: C_7\ vol.\% = \frac{C_7\ volume}{(\ C_7\ volume + Crude\ Oil\ volume\ )} * 100$$

$$**: Dilution\ ratio\ for\ nC_7\ addition = \frac{(\ C_7\ volume + Crude\ Oil\ volume\ )}{Crude\ Oil\ volume} * 100$$

Table A-2. Calculation of the corrected absorbance values after removing the effect of dilution at 1100 nm

Expected vol. % of C_7	Heptane vol. % *	A_1 = Absorbance value using air as the blank **	A_2 = Absorbance value after correction for n-heptane absorbance+	Dilution Ratio *	A_3 = Absorbance value after correction for dilution effect++
0	0.0000	1.862	1.862	1.0000	1.862
10	10.5145	1.669	1.634	1.1175	1.826
20	20.0798	1.497	1.462	1.2512	1.829
30	30.3067	1.311	1.276	1.4349	1.831
40	40.4272	1.138	1.103	1.6786	1.852
50	50.2168	1.263	1.228	2.0087	2.467
60	60.1584	2.135	2.100	2.5099	5.271
70	70.3957	2.214	2.179	3.3779	7.360
80	79.8561	1.560	1.525	4.9643	7.571
90	90.0683	0.775	0.740	10.0687	7.451

*: Taken from Table A1

**: Taken from Figure A1

+: $A_2 = A_1$ – heptane abs. at 1100 nm

++: $A_3 = A_2$ x Dilution ratio

Once the effect of n-heptane and dilution effect are corrected the absorbance data are converted into light intensity. Table A-3 presents the calculation of the light intensity as a function of the concentration of n-heptane and crude oil before and after the dilution effect correction used to study asphaltene aggregation from the

crude oil S with asphaltene concentration of 2.8 wt. % diluted with n-heptane and aged for 1 hour

Table A-3. Data processing of the light intensity before and after the removal of the dilution effect for Crude Oil S at 25°C and 1 hour aging time

Crude Oil vol. %	Heptane vol. % *	LI_1 = Light intensity before correction for n-heptane addition	LI_2 = Light intensity after correction for dilution effect	LI_3 = Normalized Light intensity after correction for dilution effect
100.00	0.00	1.37	1.37E+00	1.00E+00
89.49	10.51	2.32	1.49E+00	1.09E+00
79.92	20.08	3.45	1.48E+00	1.08E+00
69.69	30.31	5.30	1.48E+00	1.07E+00
59.57	40.43	7.89	1.41E+00	1.02E+00
49.78	50.22	5.92	3.41E-01	2.48E-01
39.84	60.16	0.79	5.36E-04	3.90E-04
29.60	70.40	0.66	4.36E-06	3.17E-06
20.14	79.86	2.99	2.69E-06	1.96E-06
9.93	90.07	18.20	3.54E-06	2.58E-06

$LI_1 = 100 * 10 \text{ ^ } (-A_2)$

$LI_2 = 100 * 10 \text{ ^ } (-A_3)$

$LI_3 = LI_{2\ /\ } LI_{2\ 100 \text{ crude oil vol.\%}}$

The previous calculations are an example for a single experiment. The results for repeated experiments are grouped and presented in the manuscript. Figure A-2 (Figure 4-1 (b)) presents the results for the light intensity LI_1 vs. crude oil vol. % and n-heptane vol. % for repeated experiments for the crude oil S aged for 1 hour and Table A-4 presents the corresponding data.

In addition Table A-5 presents the data of the results for the light intensity after the correction for the dilution effect vs. crude oil vol. % and n-heptane vol. % and Figure A-3 (Figure 4-2) presents the plot for the corresponding information. The logarithmic scale is needed to enhance the changes of the light intensity for high concentrations of n-heptane.

Table A-4. Direct spectroscopy results for Crude Oil S diluted with n-heptane and aged for 1 h at 25 ˚C

Crude Oil vol. %	Heptane, vol. %	LI_1 = Light Intensity
100.00	0	1.15
89.71	10.29	1.93
79.80	20.20	3.20
69.64	30.36	4.86
59.61	40.39	7.38
49.63	50.37	6.96
39.66	60.34	0.69
31.28	68.72	0.48
20.04	79.96	2.81
10.03	89.97	15.51

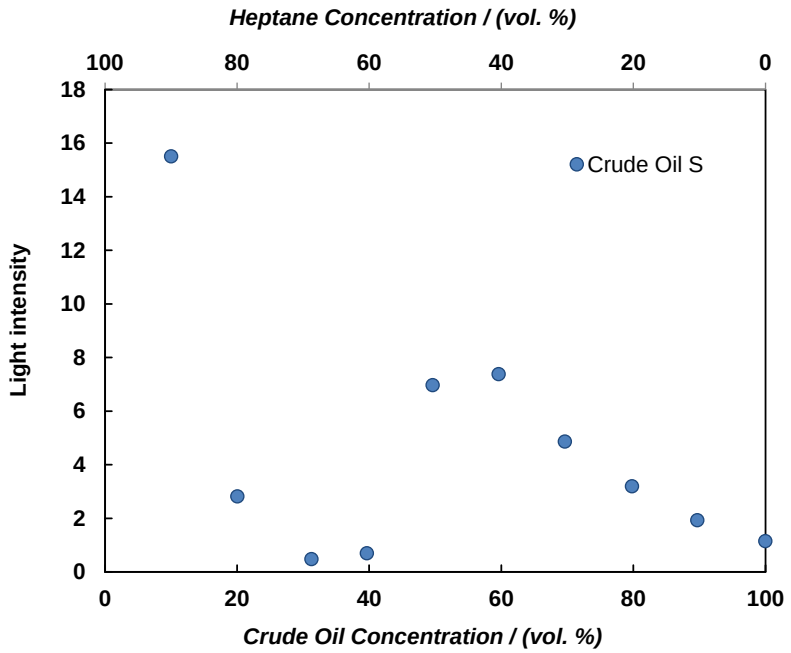

Figure A-2. (Figure 4-1 (b)) Direct spectroscopy results for Crude Oil S diluted with n-heptane and aged for 1 h at 25°C

Table A-5. Direct spectroscopy results for Crude Oil S diluted with n-heptane and aged for 1 h at 25°C. Normalized light intensity and corrected to remove the effect of dilution.

Crude Oil vol. %	Heptane, vol. %	LI_2 = Light Intensify after correction for dilution effect	LI_3 = Normalized Light intensity after correction for dilution effect
100.00	0	1.15E+00	1.00E+00
89.71	10.29	1.34E+00	1.19E+00
79.80	20.20	1.48E+00	1.34E+00
69.64	30.36	1.46E+00	1.32E+00
59.61	40.39	1.45E+00	1.32E+00
49.63	50.37	5.73E-01	5.61E-01
39.66	60.34	4.46E-04	3.88E-04
31.28	68.72	6.84E-06	6.89E-06
20.04	79.96	2.74E-06	2.49E-06
10.03	89.97	2.28E-06	1.84E-06

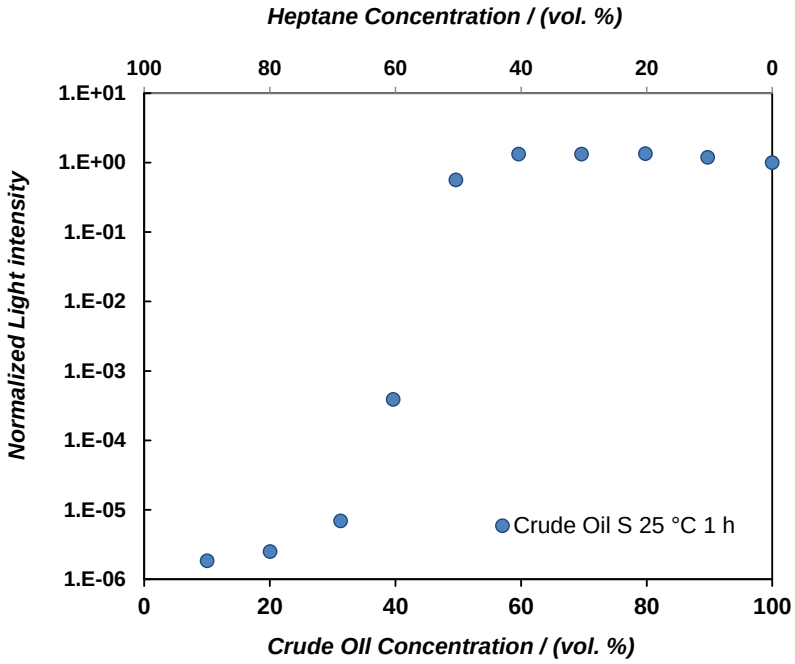

Figure A-3. (Figure 4-2) Direct spectroscopy results for Crude Oil S diluted with n-heptane and aged for 1 h at 25°C. Normalized light intensity and corrected to remove the effect of dilution